Published by Institute of Physics Publishing for SISSA/ISAS
Received: *December 2, 2003*
Revised: *January 23, 2004*
Accepted: *February 3, 2004*

Linear collider capabilities for supersymmetry in dark matter allowed regions of the mSUGRA model

Howard Baer, Alexander Belyaev and Tadas Krupovnickas

Department of Physics, Florida State University
Tallahassee, FL 32306, U.S.A.
E-mail: baer@hep.fsu.edu, belyaev@hep.fsu.edu, tadas@hep.fsu.edu

Xerxes Tata

Department of Physics and Astronomy, University of Hawaii
Honolulu, HI 96822, U.S.A.
E-mail: tata@phys.hawaii.edu

Abstract: Recent comparisons of minimal supergravity (mSUGRA) model predictions with WMAP measurements of the neutralino relic density point to preferred regions of model parameter space. We investigate the reach of linear colliders (LC) with $\sqrt{s} = 0.5$ and 1 TeV for SUSY in the framework of the mSUGRA model. We find that LCs can cover the entire stau co-annihilation region provided $\tan\beta \lesssim 30$. In the hyperbolic branch/focus point (HB/FP) region of parameter space, specialized cuts are suggested to increase the reach in this important "dark matter allowed" area. In the case of the HB/FP region, the reach of a LC extends well past the reach of the CERN LHC. We examine a case study in the HB/FP region, and show that the MSSM parameters μ and M_2 can be sufficiently well-measured to demonstrate that one would indeed be in the HB/FP region, where the lightest chargino and neutralino have a substantial higgsino component.

Keywords: Supersymmetry Phenomenology, -REM-Dark Matter, Supersymmetric Standard Model.

Contents

1. Introduction

In recent years, supersymmetric models have become increasingly constrained by a variety of measurements [1]. These include determination of the branching fraction $BF(b \to s\gamma)$ [2], the muon anomalous magnetic moment $a_\mu = (g-2)_\mu/2$ [3] and most recently, the tight restriction on the density of relic dark matter from the Big Bang, as determined by the WMAP experiment [4]. Analysis of WMAP and other data sets have determined a preferred range for the abundance of cold dark matter [4, 5]:

$$\Omega_{\mathrm{CDM}}h^2 = 0.1126^{+0.0161}_{-0.0181}\,, \qquad 2\sigma \text{ level}\,. \tag{1.1}$$

Within the minimal supergravity (mSUGRA) framework [6], the lightest neutralino is usually the lightest SUSY particle. Since R-parity is assumed to be conserved, this neutralino is stable and provides a good candidate for cold dark matter [7]. While it is possible that the relic density of neutralinos may make up almost all the cosmological dark matter, the possibility that dark matter, like visible matter, is made up of several components cannot be excluded at this point. In our analysis we will, therefore, interpret the WMAP measurement (1.1) as an *upper* bound,

$$\Omega_{\widetilde{Z}_1}h^2 < 0.129\,,$$

on the relic density in neutralinos. The mSUGRA model is characterized by four SUSY parameters together with a sign choice,

$$m_0\,, \quad m_{1/2}\,, \quad A_0\,, \quad \tan\beta \quad \text{and} \quad \mathrm{sign}(\mu)\,. \tag{1.2}$$

Here m_0 is the common mass of all scalar particles at M_{GUT}, $m_{1/2}$ is the common gaugino mass at M_{GUT}, A_0 is the common trilinear soft term at M_{GUT}, $\tan\beta$ is the ratio of Higgs field vacuum expectation values at the scale M_Z, and finally the magnitude — but not the sign — of the superpotential μ term is determined by the requirement of radiative electroweak symmetry breaking (REWSB). In addition, we take $m_t = 175\,\text{GeV}$.

The recent measurements of $\Omega_{\text{CDM}}h^2$, $BF(b \to s\gamma)$ and a_μ have considerably modified our expectations for the regions of mSUGRA model parameter space that may be realized in nature. Several years ago, relatively low values of m_0 and $m_{1/2}$ appeared to be preferred because these led to sufficiently light sleptons which in turn led to efficient neutralino annihilation in the early universe via t-channel sfermion exchange diagrams; this resulted in values of $\Omega_{\text{CDM}}h^2 < 1$, and a universe at least as old as its oldest constituents [8, 9]. The low m_0 and $m_{1/2}$ region of parameter space has been dubbed by Ellis et al. as the "bulk" annihilation region [10]. The bulk annihilation region was also favored by fine-tuning estimates in the mSUGRA model [11].

Currently, the bulk annihilation region of the mSUGRA model is disfavored by:

1. a value of m_h typically below bounds from LEP2, which require $m_h > 114.4\,\text{GeV}$ in the case of a SM-like light Higgs scalar h [12];

2. a value of $BF(b \to s\gamma)$ that is either above ($\mu < 0$) or below ($\mu > 0$) current measurements;[1]

3. for larger values of $\tan\beta$, the bulk region leads to large negative ($\mu < 0$) or large positive ($\mu > 0$) contributions to the muon magnetic dipole moment. Because of uncertainty in the SM prediction of a_μ, caution is advised in the interpretation of what the E821 data tell us about the existence of physics beyond the SM.[2]

The favored regions of mSUGRA parameter space now include [14, 15, 16]

- the stau co-annihilation region at low m_0 where $m_{\tilde{\tau}_1} \simeq m_{\widetilde{Z}_1}$, and where $\tilde{\tau}_1 - \widetilde{Z}_1$ and $\tilde{\tau}_1 - \bar{\tilde{\tau}}_1$ annihilation in the early universe also serve to reduce the neutralino relic density to sufficiently low values [17],

- the A-annihilation funnel at large $\tan\beta$ where m_H and $m_A \simeq 2m_{\widetilde{Z}_1}$ and $\widetilde{Z}_1\widetilde{Z}_1 \to A,\ H \to f\bar{f}$ (f's are SM fermions) through the very broad A and H resonances [18], and

- the hyperbolic branch/focus point region [19, 20, 21] (HB/FP) at large m_0 near the edge of parameter space where μ becomes small, and the $\widetilde{Z}_1$ has a significant higgsino component which facilitates a large annihilation rate [22, 23, 9]. The location of this region is very sensitive to the value of m_t [25].

The HB/FP region predicts multi-TeV squark and slepton masses so that supersymmetric contributions to $BF(b \to s\gamma)$ and a_μ are suppressed; these measurements are thus expected

[1] A combination of measurements from the ALEPH, BELLE and CLEO experiments yield $BF(b \to s\gamma) = (3.25 \pm 0.54) \times 10^{-4}$, while the SM prediction is $(3.6 \pm 0.3) \times 10^{-4}$ [2].

[2] In a recent analysis, Davier et al. [13] find $\Delta a_\mu = (22.1 \pm 11.3) \times 10^{-10}$ ($(7.4 \pm 10.5) \times 10^{-10}$) (errors added in quadrature) depending on whether the hadronic vacuum polarization is estimated using $e^+e^- \to hadrons$ (τ decay) data.

JHEP02(2004)007

to be close to the SM predictions. Furthermore, the relatively high scalar masses help suppress potential flavor changing and CP-violating supersymmetric processes, and offer at least a partial decoupling solution to the SUSY flavor and CP problems [20]. Finally, Feng et al. have shown that the low $m_{1/2}$ part of the hyperbolic branch has relatively low fine-tuning [20], in spite of m_0 being very large.

Given these expectations for where supersymmetry might lie, it makes sense to re-evaluate the prospects for SUSY searches at various collider and dark matter search experiments. In ref. [26], the reach of the Fermilab Tevatron for isolated trilepton events from $\widetilde{W}_1\widetilde{Z}_2$ production was extended to very large m_0 values to include the HB/FP region. In the HB/FP region, production cross sections increase due to decreased chargino and neutralino masses, but the visible energy from $\widetilde{W}_1 \to f\bar{f}'\widetilde{Z}_1$ and $\widetilde{Z}_2 \to f\bar{f}\widetilde{Z}_1$ decays also decreases, reducing detection efficiency. It was shown that the Tevatron reach in $m_{1/2}$ for isolated 3ℓ events did in fact *increase* in the HB/FP region. The reach of the CERN LHC was also worked out in ref. [27], where it was found that values of $m_{1/2} \sim 1400\,\mathrm{GeV}$ ($\sim 700\,\mathrm{GeV}$) could be probed in the stau co-annihilation region (HB/FP region) with an integrated luminosity of $100\,\mathrm{fb}^{-1}$. For higher values of $m_{1/2}$ in the HB/FP region, $m_{\tilde{g}}$ becomes very large while the visible energy from $\widetilde{W}_1$ and $\widetilde{Z}_2$ decays becomes small, so that signal detection becomes difficult. Thus, the high $m_{1/2}$ part of the hyperbolic branch currently seems beyond LHC reach. It is interesting to note that in the HB/FP region of the mSUGRA model, the higgsino component of the $\widetilde{Z}_1$ is sufficiently large to yield direct neutralino-nucleus scattering rates within the reach of Stage 3 direct dark matter detection experiments such as Genius, Cryoarray and Zeplin-4 [28]. In addition, in the HB/FP region one may expect detectable rates for detection of neutrinos arising from neutralino annihilation in the core of the sun or the earth, and also large rates for cosmic photons, positrons and antiprotons due to DM annihilation in the galactic halo [23, 24].

In the HB/FP region, since $|\mu|$ becomes small, charginos are light. This then implies that there would be a large rate for chargino pair production at e^+e^- linear colliders (LCs) operating with center-of-mass energy $\sqrt{s} \simeq 0.5 - 1\,\mathrm{TeV}$ over most of the HB/FP region. However, since the $\widetilde{W}_1 - \widetilde{Z}_1$ mass gap also becomes small, it is not clear that linear collider experiments would access the entire kinematically allowed chargino pair production region.

Our main goal in this paper is to assess the reach of linear colliders for SUSY in the mSUGRA model [29, 30], paying particular attention to the HB/FP region. We note here that previous reach estimates of linear colliders for SUSY in the mSUGRA model extended only up to m_0 values as high as 800 GeV [29]– well below the HB/FP region. We find that a linear collider, using standard cuts for chargino pair events, can explore the low $m_{1/2}$ portion of the HB/FP region. To explore the high $m_{1/2}$ part of the hyperbolic branch, new specialized cuts are suggested. With these cuts, it appears possible to probe essentially all of the HB/FP region (up to $m_{1/2} = 1.6\,\mathrm{TeV}$) where charginos satisfy the LEP2 bounds, and where chargino pairs are kinematically accessible at a linear collider (LC). This then provides the first example of a SUSY parameter space region which is accessible to linear e^+e^- colliders, while likely remaining out of reach of LHC experiments! This is especially interesting since the HB/FP region is one of the three qualitatively different mSUGRA parameter space regions allowed by dark matter and other constraints.

JHEP02(2004)007

If indeed a SUSY signal from charginos is detected, the next step would be to try and determine the associated weak scale parameters: μ, M_2 and $\tan\beta$ [31]. We explore a particular case study in the low $m_{1/2}$ region of the HB/FP region, and show that at least in this case μ and M_2 should be measurable. This measurement would give a firm indication of the large higgsino content of the light chargino and $\widetilde{Z}_1$ and, together with the fact that sfermions are not detected either at the LC or at the LHC, provide a strong indication that SUSY in fact lies in the HB/FP region.

The remainder of this paper is organized as follows. In section 2, we examine the problems associated with detecting SUSY in mSUGRA parameter space at an e^+e^- LC, with special emphasis on the HB/FP region, and show that these can be overcome. We propose novel cuts that allow the large $m_{1/2}$ part of the hyperbolic branch to be explored via chargino pair production. We then show our projections for the SUSY reach of a LC operating at $\sqrt{s} = 0.5\,\text{TeV}$ or $\sqrt{s} = 1\,\text{TeV}$, assuming $100\,\text{fb}^{-1}$ of integrated luminosity. In section 3, we compare the reach of a LC with the reach of Fermilab Tevatron luminosity upgrades and of the CERN LHC. Furthermore, we also show the dark matter allowed region of mSUGRA parameter space to elucidate the performance of these experiments in this preferred region of parameter space. In section 4, we perform a case study in the HB/FP region, where chargino pair production is accessible to a $\sqrt{s} = 0.5\,\text{TeV}$ LC. The masses $m_{\widetilde{W}_1}$ and $m_{\widetilde{Z}_1}$ can be measured via energy distribution end-points. We find that these measurements, along with measurement of the total chargino pair cross section, allow a determination of the underlying SUSY parameters μ and M_2, although $\tan\beta$ remains relatively undetermined. In section 5, we present our conclusions.

2. Reach of a linear collider in the mSUGRA model

In our signal and background computations, we use ISAJET 7.69 [32] which allows for the use of polarized beams, and also allows for convolution of subprocess cross sections with electron parton distribution functions (PDFs) arising from both initial state bremsstrahlung and also beamstrahlung [33]. We use the ISAJET toy detector CALSIM with calorimetry covering the regions $-4 < \eta < 4$ with cell size $\Delta\eta \times \Delta\phi = 0.05 \times 0.05$. Electromagnetic energy resolution is given by $\Delta E_{\rm em}/E_{\rm em} = 0.15/\sqrt{E_{\rm em}} \oplus 0.01$, while hadronic resolution is given by $\Delta E_h/E_h = 0.5\sqrt{E_h} \oplus 0.02$, where $\oplus$ denotes addition in quadrature. Jets are identified using the ISAJET jet finding algorithm GETJET using a fixed cone size of $\Delta R = \sqrt{\Delta\eta^2 + \Delta\phi^2} = 0.6$, modified to cluster on energy rather than transverse energy. Clusters with $E > 5\,\text{GeV}$ and $|\eta(jet)| < 2.5$ are labeled as jets. Muons and electrons are classified as isolated if they have $E > 5\,\text{GeV}$, $|\eta_\ell| < 2.5$, and the visible activity within a cone of $R = 0.5$ about the lepton direction is less than $\max(E_\ell/10\,\text{GeV}, 1\,\text{GeV})$. Finally, jets originating from b-quarks are tagged as b-jets with an efficiency of 50%.

2.1 Review of previous reach assessment

The reach of a $\sqrt{s} = 0.5\,\text{TeV}$ LC for supersymmetry has previously been evaluated in ref. [29] assuming an integrated luminosity of $20\,\text{fb}^{-1}$. Reach contours were presented for the case of the mSUGRA model in the m_0 vs. $m_{1/2}$ plane for $A_0 = 0$, $\tan\beta = 2$ and 10, and $\mu \gtrless 0$. The reach plots in that study were limited to $m_{1/2} < 600\,\mathrm{GeV}$ and $m_0 < 800\,\mathrm{GeV}$, i.e. well outside the HB/FP region.

The region of the $m_0 - m_{1/2}$ plane where there should be an observable SUSY signal in LC experiments consists of three distinct pieces.

- At low m_0 with $m_{1/2} \sim 300 - 500\,\mathrm{GeV}$, slepton pair production occurs at large rates. The signal is a pair of opposite sign/same flavor leptons plus missing energy. Tsukamoto et al. [31] suggested cuts of (i) $5\,\mathrm{GeV} < E(\ell) < 200\,\mathrm{GeV}$, (ii) $20\,\mathrm{GeV} < E_{vis.} < \sqrt{s} - 100\,\mathrm{GeV}$, (iii) $|m(\ell\bar{\ell}) - M_Z| > 10\,\mathrm{GeV}$, (iv) $|\cos\theta(\ell^\pm)| < 0.9$, (v) $-Q_\ell \cos\theta_\ell < 0.75$, (vi) $\theta_{\rm acop} > 30°$, (vii) $E_T^{\rm mis} > 25\,\mathrm{GeV}$ and (viii) veto events with any jet activity. Here, $\theta_{\rm acop} \equiv \pi - \cos^{-1}(\hat{p}_x^+\hat{p}_x^- + \hat{p}_y^+\hat{p}_y^-)$. The reach was evaluated by running with right-polarized electron beams where $P_L(e^-) = -0.9$. The beam polarization maximizes $\tilde{\ell}_R\bar{\tilde{\ell}}_R$ pair production, while minimizing background from W^+W^- production.

- At low $m_{1/2}$ values, chargino pair production occurs at a large rate. To search for chargino pairs, one may look for $1\ell + 2j + E^{\rm mis}$ events. Following ref. [31], it was required in ref. [29] to have one isolated lepton plus two jets with (i) $20\,\mathrm{GeV} < E_{vis} < \sqrt{s} - 100\,\mathrm{GeV}$, (ii) if $E_{jj} > 200\,\mathrm{GeV}$, then $m(jj) < 68\,\mathrm{GeV}$, (iii) $E_T^{\rm mis} > 25\,\mathrm{GeV}$, (iv) $|m(\ell\nu) - M_W| > 10\,\mathrm{GeV}$ for a W pair hypothesis, (v) $|\cos\theta(j)| < 0.9$, $|\cos\theta(\ell)| < 0.9$, $-Q_\ell\cos\theta_\ell < 0.75$ and $Q_\ell\cos\theta(jj) < 0.75$, (vi) $\theta_{\rm acop}(WW) > 30°$ for a W pair hypothesis. The reach for $1\ell + 2j + \not{E}_T$ events from chargino pair production was evaluated using a left polarized beam with $P_L = +0.9$.

- Finally, there exists a small region around $m_0 \sim 200 - 500\,\mathrm{GeV}$ and $m_{1/2} \sim 300 - 350\,\mathrm{GeV}$ where neither slepton pairs nor chargino pairs are kinematically accessible, but where $e^+e^- \to \widetilde{Z}_1\widetilde{Z}_2$ is. In this case, the decay $\widetilde{Z}_2 \to \widetilde{Z}_1 h$ was usually found to be dominant. Since $h \to b\bar{b}$ with a large branching fraction, $b\bar{b} + \not{E}_T$ events were searched for with two tagged b-jets, $E_T^{\rm mis} > 25\,\mathrm{GeV}$ and $30° < \Delta\phi_{b\bar{b}} < 150°$. Imposing a missing mass cut $\not{m} > 340\,\mathrm{GeV}$ eliminated almost all SM backgrounds, so that a signal cross section of 10 fb would yield 10 signal events for integrated luminosity $20\,\mathrm{fb}^{-1}$, where the signal efficiency was found to be 6%. Beam polarization of $P_L = +0.9$ was used.

In the following, we refer to these as the "standard cuts".

The ultimate reach contours found in ref. [29] generally track the boundary of the kinematically allowed regions for $\widetilde{W}_1$ and $\tilde{e}_R$ pair production. An exception occurs at low m_0 values where selectron pair production is dominant, but where $m_{\tilde{e}_R} \simeq m_{\widetilde{Z}_1}$. Then, the mass gap $m_{\tilde{e}_R} - m_{\widetilde{Z}_1}$ becomes so small that there was very little visible energy in the slepton pair events, resulting in very low detection efficiency, causing a turnover in the reach contours. For $\tan\beta$ values larger than those explored in ref. [29], the large τ Yukawa coupling makes $\tilde{\tau}_1$ significantly lighter than $\tilde{e}_R$ so that close to the boundary of excluded region at small m_0 $\tilde{e}_R\bar{\tilde{e}}_R$ events may still be observable, while $\tilde{\tau}_1\bar{\tilde{\tau}}_1$ events are not.

JHEP02(2004)007

2.2 Updated reach results

In this section, we update our earlier reach projections [29] for a linear collider. We present reach projections for linear colliders with $\sqrt{s} = 0.5$ and 1 TeV of energy in the CM frame. We also expand the range of $m_{1/2}$ (to 1.6 TeV) and m_0 (to 8 TeV) beyond the values presented in ref. [29]. This allows us to explore the entire stau co-annihilation strip, the A-annihilation funnel and the HB/FP region. In our analysis, we restrict ourselves to the trilinear SSB term $A_0 = 0$. For the most part, our results are qualitatively insensitive to variations in A_0. An exception occurs for particular A_0 choices which may greatly reduce the value of $m_{\tilde{t}_1}$, and lead to a top squark-neutralino co-annihilation region [34].

Our first results are presented in figure 1, where we show the m_0 vs. $m_{1/2}$ plane for $\tan\beta = 30$, $\mu > 0$ and $A_0 = 0$. The left-most red region at low m_0 is disallowed because the LSP would become a stau. The right-most red region (large m_0) is mainly excluded by a lack of appropriate REWSB, although this includes as well points with no convergent

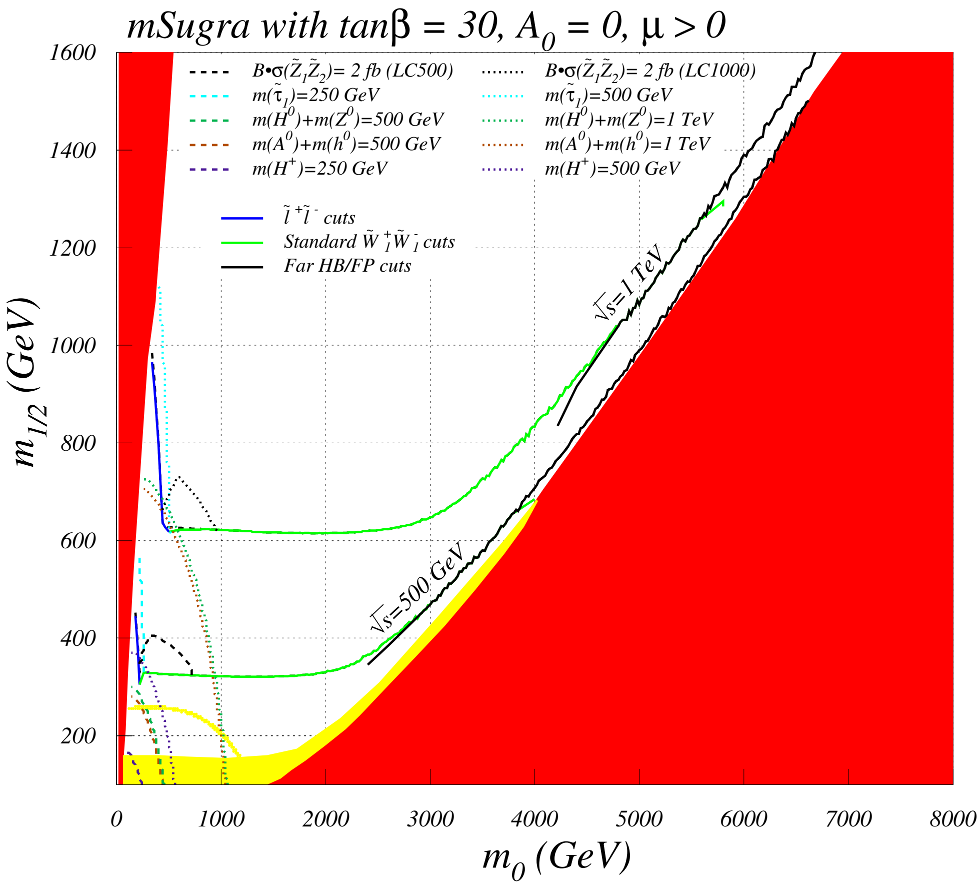

Figure 1: Reach of a linear collider for supersymmetry in the mSUGRA model for $\sqrt{s} = 500$ and 1000 GeV, for $\tan\beta = 30$, $A_0 = 0$ and $\mu > 0$. The reach via slepton pair production is denoted by the blue contour, while standard cuts for chargino pair production yield the green contour. Special chargino pair cuts yield the black contour in the HB/FP region. The red region is theoretically excluded, while the yellow region is excluded by LEP2 measurements. Below the yellow contour, $m_h \leq 114.4$ GeV.

RGE solution as generated by ISAJET. The precise location of the boundary of the large m_0 red region depends somewhat on the computer code, and also on the assumed fermion masses. The lower yellow region is excluded by LEP2 chargino searches, which require $m_{\widetilde{W}_1} > 103.5\,\mathrm{GeV}$. In addition, the region below the yellow contour gives a light (SM-like) Higgs boson with $m_h < 114.4\,\mathrm{GeV}$.

Using the standard dilepton cuts as described above, we find a SM background level of $\sigma_{SM} = 1.79\,\mathrm{fb}$ (0.045 fb) for a LC with $\sqrt{s} = 0.5\,\mathrm{TeV}$ (1.0 TeV) with right polarized beams using $P_L(e^-) = -0.9$.[3] It has been shown in ref. [31] that backgrounds from $2 \to 3$ processes such as $e^+e^- \to \nu\nu Z, e^+e^- Z$ or $e^\pm \nu W^\mp$ production or $2 \to 4$ processes such as $e^+e^- \to W^+W^-$ production are also efficiently removed by these cuts, at least for $\sqrt{s} = 500\,\mathrm{GeV}$. Although the cross sections for these processes grow with energy, we expect that these cuts will remove the *bulk* of these backgrounds also at $\sqrt{s} = 1000\,\mathrm{GeV}$; for instance, the dominant portion of the $eeWW$ background that comes from "$\gamma\gamma$" collisions will be removed by the acoplanarity and other cuts; much of the remaining cross section will have $p_T(WW) \leq M_W$ and will also be reduced, though not eliminated by these cuts. However, since these backgrounds have not been included in our evaluation it is possible that the statistical significance of the signal may be somewhat over-estimated for $\sqrt{s} = 1000\,\mathrm{GeV}$. The regions to the left of the lower (upper) blue contour yield a supersymmetric signal at the 5σ level assuming $100\,\mathrm{fb}^{-1}$ of integrated luminosity at the 0.5 (1) TeV LC. An increased reach for slepton pairs may be obtained by searching for ditau events originating from stau pair production. While we did not perform a detailed signal-to-background analysis for this channel, we do show the kinematic limit for stau pair production by a dashed light-blue contour, which for $\tan\beta = 30$, lies somewhat above the blue dilepton reach contour. Thus, a significant gain in reach might be acquired by searching for acollinear di-tau events arising from stau pair production. In particular, this signal may give access to the large $m_{1/2}$ part of the stau co-annihilation region.

The green contour denotes the reach of a 0.5 or 1 TeV LC for SUSY via the $1\ell+2j+\not{E}_T$ channel arising from chargino pair production, using the standard cuts given above. Unlike ref. [29], we use $P_L = 0$, and find a background level of 15.5 fb (2.1 fb) for $\sqrt{s} = 0.5$ (1) TeV (the beam polarization is not important for this reach contour). For most of parameter space, the reach contours follow closely along the $m_{\widetilde{W}_1} = 250$ (500) GeV mass contours, indicating that chargino pair production can be seen with standard cuts almost to the kinematical limit for chargino pair production. An exception occurs when m_0 becomes very large, in the HB/FP region. Around $m_0 \sim 4000\,\mathrm{GeV}$ ($m_0 \sim 6000\,\mathrm{GeV}$) for $\sqrt{s} = 0.5\,\mathrm{TeV}$ (1 TeV), the reach contour departs from the kinematic limit. The termination of the reach contour occurs because in this region, the superpotential parameter μ becomes very small, and the light chargino $\widetilde{W}_1$ and neutralino $\widetilde{Z}_1$ become higgsino-like, and increasingly mass degenerate. The Q-value from $\widetilde{W}_1 \to \widetilde{Z}_1 f\bar{f}'$ decay (the fs are light SM fermions) becomes very small, and very little visible energy is released by the chargino decays. This causes the detection efficiency for $1\ell + 2j+\not{E}_T$ events to decrease sharply, leading to a corresponding reduction in the reach using the standard cuts.

[3]In our assessment of SM backgrounds, we have evaluated only the backgrounds from $2 \to 2$ processes.

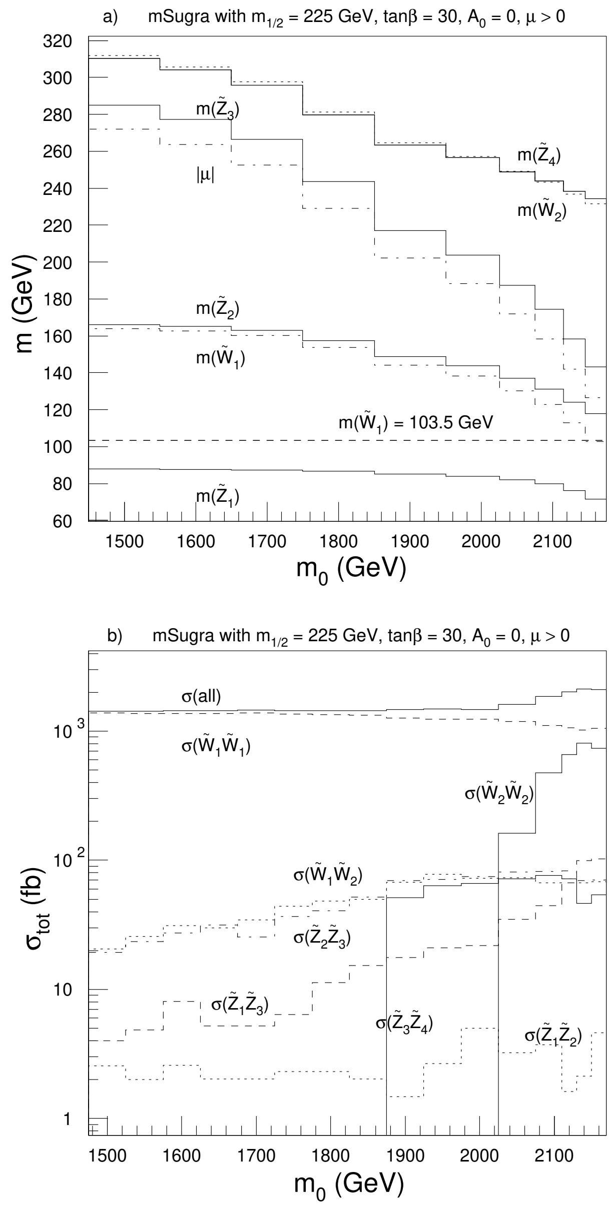

Figure 2: Plot of (a). sparticle masses and (b). sparticle pair production cross sections versus m_0 in the HB/FP region for $m_{1/2} = 225\,\mathrm{GeV}$, $\tan\beta = 30$, $A_0 = 0$ and $\mu > 0$ for a $\sqrt{s} = 500\,\mathrm{GeV}$ e^+e^- collider.

To understand what is happening in the HB/FP region, we show relevant sparticle masses in figure 2a for $m_{1/2} = 225\,\mathrm{GeV}$, $\tan\beta = 30$, $A_0 = 0$ and $\mu > 0$ versus the parameter m_0. As m_0 varies from 1400 GeV to nearly 2200 GeV, i.e. as we approach the HB/FP region for fixed $m_{1/2}$ with increasing m_0. As m_0 increases, $|\mu|$ is seen to be decreasing. Since the value of SU(2) gaugino mass M_2 is essentially fixed, the various chargino and neutralino masses also decrease, with the lighter ones becoming increasingly higgsino-like. The plot is terminated when the LEP2 limit $m_{\widetilde{W}_1} \geq 103.5\,\mathrm{GeV}$ is reached. Of great importance is that the $\widetilde{W}_1 - \widetilde{Z}_1$ mass gap is also decreasing, although in this case it remains substantial out to the edge of parameter space.

In figure 2b, we show the total cross section for various chargino and neutralino production reactions versus m_0 as in frame (a). At the lower m_0 values, $\sigma(\widetilde{W}_1^+\widetilde{W}_1^-)$ pair production dominates the total SUSY production cross section. As m_0 increases, and $|\mu|$ decreases, the other charginos and neutralinos become light as well, and many more reactions "turn on" in the HB/FP region. Although we will focus mainly on $\widetilde{W}_1^+\widetilde{W}_1^-$ pair production, it is important to note that many SUSY production reactions can occur in the HB/FP region, and can lead to an assortment of SUSY events from the production and cascade decays of the heavier chargino and neutralino states.

A similar plot is shown in figure 3, except this time for $m_{1/2} = 900\,\mathrm{GeV}$, i.e. in the upper regions of the hyperbolic branch. In this case, M_2 is much larger than the case shown in figure 2, and so the heavier charginos and neutralinos remain inaccessible to a LC. As m_0 increases, again $m_{\widetilde{W}_1}$ and $m_{\widetilde{Z}_1}$ decrease.[4] But in this case the $\widetilde{W}_1 - \widetilde{Z}_1$ mass gap is much smaller, reaching only several GeV at the limit of parameter space. Clearly, in this upper $m_{1/2}$ region of the hyperbolic branch, there will be little visible energy emerging from chargino 3-body decays, making detection of chargino pair events difficult using standard cuts. In addition, as shown in frame (b), only $\widetilde{W}_1^+\widetilde{W}_1^-$ and $\widetilde{Z}_1\widetilde{Z}_2$ pair production occur, so fewer anomalous events are expected in the upper HB/FP region. Since $m_{\widetilde{Z}_2} \sim m_{\widetilde{W}_1}$, there will also be little visible energy from $\widetilde{Z}_2 \to \widetilde{Z}_1 f\bar{f}$ decay, so that $\widetilde{Z}_1\widetilde{Z}_2$ production will also be more difficult to observe. In the deep HB/FP region where $|\mu| \ll M_{1,2}$, one of the neutralinos is mainly higgsino-like with roughly equal components of $\tilde{h}_u$ and $\tilde{h}_d$. The other neutralinos, being orthogonal to these, thus either have equal magnitudes for their $\tilde{h}_u$ and $\tilde{h}_d$ content, or this content is small. In either case, the $Z\widetilde{Z}_i\widetilde{Z}_i$ coupling is dynamically suppressed [35] in this region. This accounts for the strong suppression of $\sigma(\widetilde{Z}_2\widetilde{Z}_2)$ (recall that the electron sneutrino is very heavy) in figure 3b.

Coincidentally, the reach of a $\sqrt{s} = 0.5\,\mathrm{TeV}$ LC in the $1\ell + 2j + \not{E}_T$ channel using the standard cuts terminates in the HB/FP region at nearly the same $m_{1/2}$ value as does the reach of the CERN LHC shown in ref. [27], and again in section 4 of this paper. Meanwhile, the contour of chargino pair kinematic accessibility extends to much higher $m_{1/2}$ values, along the hyperbolic branch. This motivated us to examine strategies to extend the reach of a LC to the large $m_{1/2}$ part of the HB/FP region.

To find better suited signal selection cuts for the HB/FP region, we examine a particular case study for the mSUGRA point which is beyond the projected reach of the LHC [27]:

$$m_0 = 4625\,\mathrm{GeV}\,, \quad m_{1/2} = 885\,\mathrm{GeV}\,, \quad A_0 = 0\,, \quad \tan\beta = 30\,, \quad \mathrm{sign}(\mu) = +1\,, \tag{2.1}$$

for which various sparticle masses and parameters are listed in table 1. We will refer to this as case 1. Not only is this point inaccessible at the LHC, but most of the sparticles are also inaccessible to a LC, with the exception being the lighter charginos and neutralinos. While

[4] Since $|\mu|$ decreases very rapidly as m_0 increases and approaches the theoretical boundary of the HB/FP region, its precise value is not easy to obtain using numerical methods. The value of μ, of course, directly affects the chargino and neutralino masses. In this figure, we have smoothed out what appeared to be rather large numerical fluctuations in two of the bins.

JHEP02(2004)007

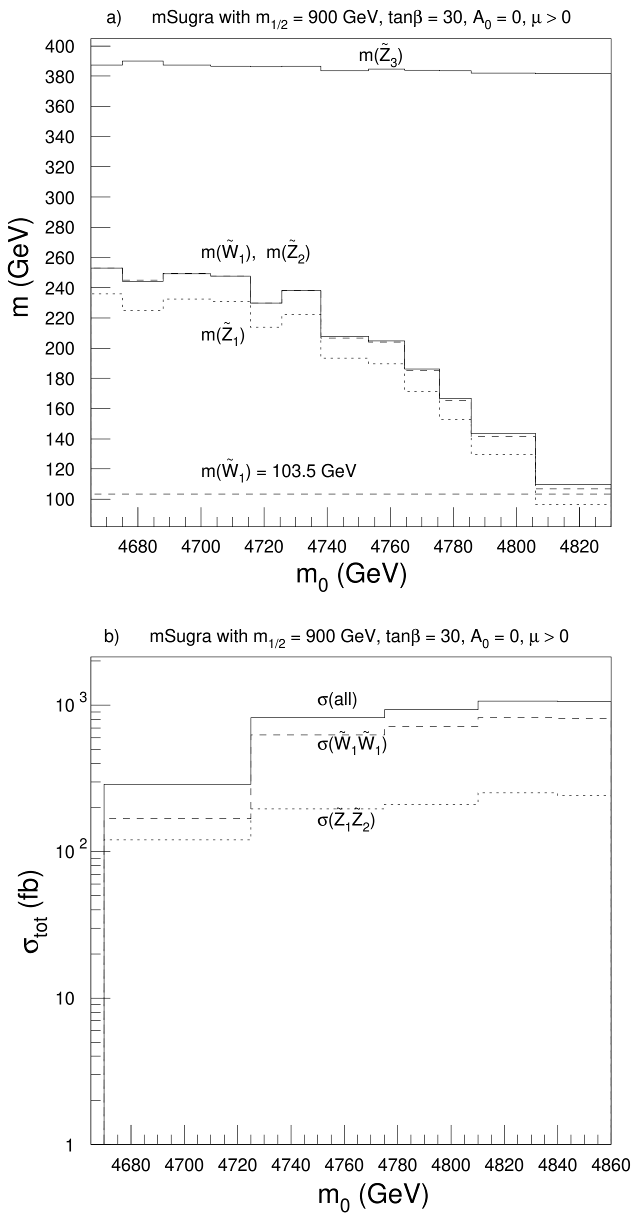

Figure 3: Plot of (a). sparticle masses and (b). sparticle pair production cross sections versus m_0 in the HB/FP region for $m_{1/2} = 900\,\mathrm{GeV}$, $\tan\beta = 30$, $A_0 = 0$ and $\mu > 0$ for a $\sqrt{s} = 500\,\mathrm{GeV}$ e^+e^- collider.

$m_{\widetilde{W}_1} = 195.8\,\mathrm{GeV}$, so that $\widetilde{W}_1^+\widetilde{W}_1^-$ pair production occurs at a large rate at a $\sqrt{s} = 0.5\,\mathrm{TeV}$ e^+e^- collider, the $\widetilde{W}_1 - \widetilde{Z}_1$ mass gap is only $14.2\,\mathrm{GeV}$, so little visible energy is released in chargino pair production events.

With this in mind, we generate SUSY events for this case study using ISAJET 7.69 for a linear collider with $\sqrt{s} = 0.5\,\mathrm{TeV}$ and unpolarized beams, including bremsstrahlung and beamstrahlung for background events. The beamstrahlung parameters, defined in ref. [33], are taken to be $\Upsilon = 0.1072$ with beam length $\sigma_z = 0.12\,\mathrm{mm}$.

In figure 4a we show the distribution of $E_{\rm visible}$ from events with 1-lepton and two jets expected at a $\sqrt{s}=$ 500 GeV LC. The solid black histogram represents the SUSY case study, which peaks at very low $E_{\rm visible}$, as expected from the low energy release from chargino decays. The small number of events around $E_{\rm visible}=250$ GeV is from Zh production. The green histogram shows the sum of all $2\to 2$ SM backgrounds as generated by ISAJET. The large $E_{\rm visible}$ component of these arises from WW, ZZ and $t\bar{t}$ production, where some energy is lost due to associated neutrino emissions. The SM background distribution extends to low $E_{\rm visible}$ values, and has a visible shoulder at $E_{\rm visible}\sim M_Z$ due to processes such as $e^+e^-\to Z\to b\bar{b}, c\bar{c}$, where the Z can be made by convoluting the subprocess reaction with the electron PDF, and the lepton from the decay of the heavy flavor is accidently isolated. The bulk of the $2\to 2$ SM background can be eliminated by requiring low values of $E_{\rm visible}$. In this case we require

$$20\,{\rm GeV} < E_{\rm visible} < 100\,{\rm GeV}\,. \tag{2.2}$$

parameter	value (GeV)
M_2	705.8
M_1	372.2
μ	185.9
$m_{\tilde{g}}$	2182.7
$m_{\tilde{u}_L}$	4893.9
$m_{\tilde{e}_L}$	4656.1
$m_{\widetilde{W}_1}$	195.8
$m_{\widetilde{W}_2}$	743.5
$m_{\widetilde{Z}_1}$	181.6
$m_{\widetilde{Z}_2}$	196.2
$m_{\widetilde{Z}_3}$	377.3
$m_{\widetilde{Z}_4}$	760.0
m_A	3998.3
m_h	122.0
$\Omega_{\widetilde{Z}_1}h^2$	0.0104
$BF(b\to s\gamma)$	3.34×10^{-4}
Δa_μ	0.6×10^{-10}

Table 1: Masses and parameters in GeV units for case 1 for $m_0=4625$ GeV, $m_{1/2}=885$ GeV, $A_0=0$, $\tan\beta=30$, ${\rm sign}\,\mu=+1$ in the mSUGRA model. The spectrum is obtained using ISAJET v7.69.

The upper limit is chosen to be well above the case 1 signal distribution endpoint to accommodate later scans over all mSUGRA parameter space, including points which allow larger $\widetilde{W}_1-\widetilde{Z}_1$ mass gaps, and somewhat harder $E_{\rm visible}$ distributions. We also show a red histogram which shows the results of the evaluation of the background from $e^+e^-\to e^+e^-c\bar{c}$, $e^+e^-b\bar{b}$ processes when both initial leptons escape detection when being scattered at a very small angle. We evaluated this background, which mainly arises from photon photon collisions, using the PYTHIA event generator [36]. In the case of $b\bar{b}$ production, the isolated lepton arises from semi-leptonic $b\to c\ell\nu$ decay, and the jets come one from a b quark, and the other from the charm quark.

In $\gamma\gamma\to b\bar{b}$ events, the b and $\bar{b}$ will typically emerge back-to-back in the transverse plane. Thus, in figure 4b we plot the distribution in $\cos\phi(jj)$, where $\phi(jj)$ is the transverse dijet opening angle. The signal is distributed over a range of $\cos\phi(jj)$ values, and actually peaks at $\cos\phi(jj)\sim 1$. The background peaks at $\cos\phi(jj)\sim -1$, so we require a cut of

$$\cos\phi(jj) > -0.6\,. \tag{2.3}$$

Finally, any surviving background arising from $b\bar{b}$ or $c\bar{c}$ production followed by semileptonic heavy flavor decay is likely to have a jet-lepton invariant mass bounded by the heavy flavor mass (at least at parton level). In figure 4c we show the distribution in $m(\ell j)$ where we form the invariant mass from the jet which is closest to the isolated lepton in space angle. Some additional background removal at low cost to signal is gained by requiring

$$m(\ell j_{\rm near}) > 5\,{\rm GeV}\,. \tag{2.4}$$

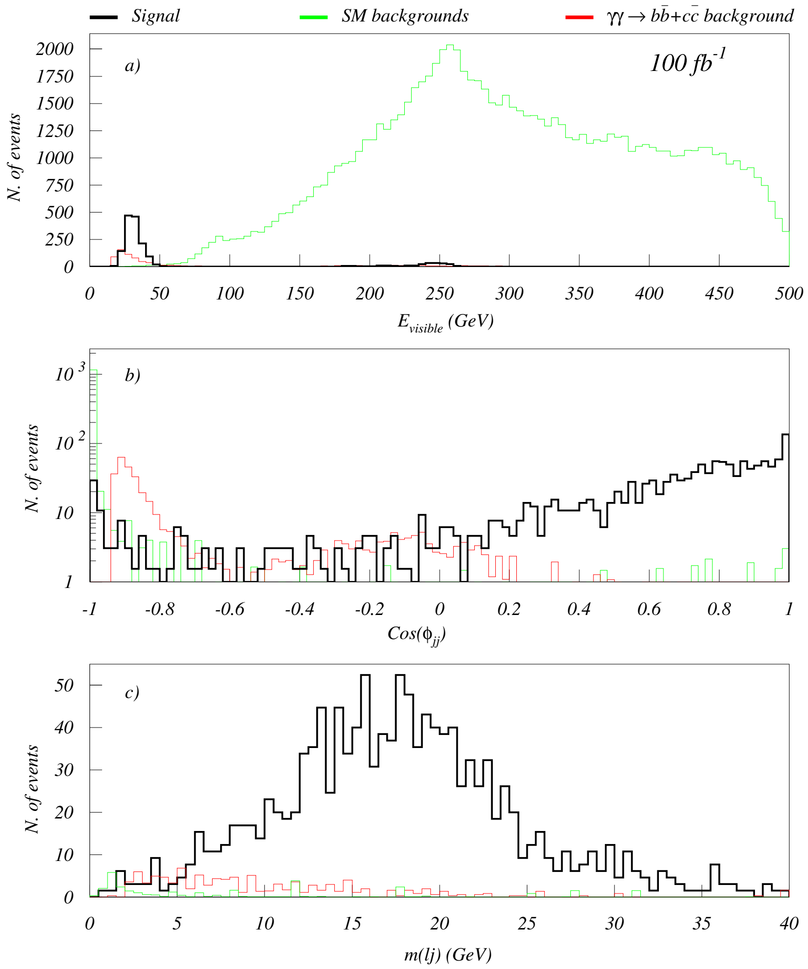

Figure 4: Distribution in (a) $E_{\rm visible}$ for mSUGRA signal (black histogram) with ($m_0 = 4625\,$GeV, $m_{1/2} = 885\,$GeV, $A_0 = 0$, $\tan\beta = 30$, sign$(\mu) = 1$) after cuts in the first row of table 2. We take $\sqrt{s} = 500\,$GeV and an integrated luminosity of $100\,\mathrm{fb}^{-1}$, and adopt beamstrahlung parameters $\Upsilon = 0.1072$ and $\sigma_z = 0.12\,$mm. The ISAJET SM background is shown by the green histogram, while the background from $\gamma\gamma \to c\bar{c}$, $b\bar{b}$ is shown in red. In (b), we show the distribution in transverse plane dijet opening angle requiring, in addition, that $20\,\mathrm{GeV} < E_{\rm visible} < 100\,$GeV. In (c), we show the distribution in $m(\ell j)$, after the aditional requirement $\cos\phi(jj) > -0.6$. The jet entering the $m(\ell j)$ distribution is the one that is closest in angle to the lepton direction.

At this point, the distribution is clearly dominated by signal. The cross sections in fb after each cut for signal and background are shown in table 2, where we include in addition background from the $2 \to 4$ process $e^+e^- \to \ell\nu q\bar{q}'$ (evaluated using CompHEP [37]). In the $2 \to 4$ calculation we eliminate Feynman diagrams such as WW pair production which are already accounted for as $2 \to 2$ processes in ISAJET. The $2 \to 4$ processes are negligible after the $E_{\rm visible}$ cut. For all frames of figure 4 we have assumed $100\,\mathrm{fb}^{-1}$ total integrated luminosity. We recognize that the dominant background to the rather soft signal which comes from two photon collisions will be sensitive to the beamstrahlung parameters, and

JHEP02(2004)007

cuts	case 1	ISAJET BG	$\gamma\gamma \to c\bar{c}, b\bar{b}$	$\ell\nu q\bar{q}'$
η, E, ΔR	16.2	897.1 (483)	9.2 (6.2)	448 (712)
$20\,\mathrm{GeV} < E_{\mathrm{vis}} < 100\,\mathrm{GeV}$	14.4	12.6 (3.5)	5.4 (4.9)	0.16 (0.08)
$\cos\phi(jj) > -0.6$	13.5	0.34 (0.2)	1.1 (1.1)	0.04 (0.02)
$m(\ell j) > 5\,\mathrm{GeV}$	12.9	0.17 (0.1)	0.8 (0.8)	0.04 (0.02)

Table 2: Cross section after cuts in fb for mSUGRA case 1 signal and ISAJET SM backgrounds, two photon background $\gamma\gamma \to c\bar{c}$, $b\bar{b}$ and the $2 \to 4$ process $e^+e^- \to \ell\nu_\ell q\bar{q}'$. We take $\sqrt{s} = 0.5\,\mathrm{TeV}$ collider CM energy. The corresponding background for $\sqrt{s} = 1\,\mathrm{TeV}$ case is listed in parenthesis.

hence to the shape of the beams. Nevertheless, the large signal to background ratio that we find encourages us to expect that our conclusions about the large reach of LC will be qualitatively unaltered.

We now require a 5σ signal for SUSY events above the total SM background as listed in table 2, for $100\,\mathrm{fb}^{-1}$ of integrated luminosity and scan mSUGRA points in the HB/FP region of figure 1. The new result is the black contour, below which the mSUGRA parameter space is accessible by the LC at 5σ level. One can see that this contour pushes the reach of the LC to much higher values of $m_{1/2}$. The contour peters out at low $m_{1/2}$ values, where the visible energy arising from chargino pair production is typically much higher than the 100 GeV maximum required by our cuts. However, this low $m_{1/2}$ region is already well covered by the standard chargino search cuts listed at the beginning of this section. The new cuts for the far HB/FP region work for e^+e^- colliders with $\sqrt{s} = 1\,\mathrm{TeV}$ as well. The $\sqrt{s} = 1\,\mathrm{TeV}$ reach contour extends even beyond the limits of parameter space shown in figure 1.

To complete our SUSY reach contours, we also examined the reach of a LC for SUSY via the $e^+e^- \to \widetilde{Z}_1\widetilde{Z}_2$ reaction in the non-HB/FP part of parameter space, where neither chargino pair production nor slepton pair production is kinematically accessible. In this case, we follow ref. [29] in asking for $b\bar{b}+\not{E}_T$ events from $e^+e^- \to \widetilde{Z}_1\widetilde{Z}_2$ production followed by $\widetilde{Z}_2 \to \widetilde{Z}_1 h$, where $h \to b\bar{b}$. In ref. [29], no background was found after a series of cuts listed at the beginning of this section. Here, we do not perform complete event generation at every point in parameter space, but instead require that

$$\sigma(e^+e^- \to \widetilde{Z}_1\widetilde{Z}_2) \times BF(\widetilde{Z}_2 \to \widetilde{Z}_1 h) > 2\,\mathrm{fb}\,, \tag{2.5}$$

which should yield ~ 10 signal events for $100\,\mathrm{fb}^{-1}$ of integrated luminosity assuming an efficiency of $5 - 6\%$ as found in ref. [29]. The resulting reach contour is shown in figure 1 as the black contour linking the slepton pair reach to the chargino reach contour. It gives some additional parameter space reach to a LC, although it is in a dark matter *disfavored* region of parameter space (unless $\tan\beta$ is large, and the H, A-annihilation funnel cuts through it). There is a turnover in the $e^+e^- \to \widetilde{Z}_1\widetilde{Z}_2$ reach contour at low m_0; this occurs because in this region, $\widetilde{Z}_2 \to \tilde{\tau}_1\bar{\tau}$ decay becomes accessible, resulting in a suppression of the $\widetilde{Z}_2 \to \widetilde{Z}_1 h$ branching fraction. However, the $\widetilde{Z}_2 \to \tilde{\tau}_1\bar{\tau}$ signal may also be detectable; if so, the gap caused by the turn-over just mentioned would be filled.

JHEP02(2004)007

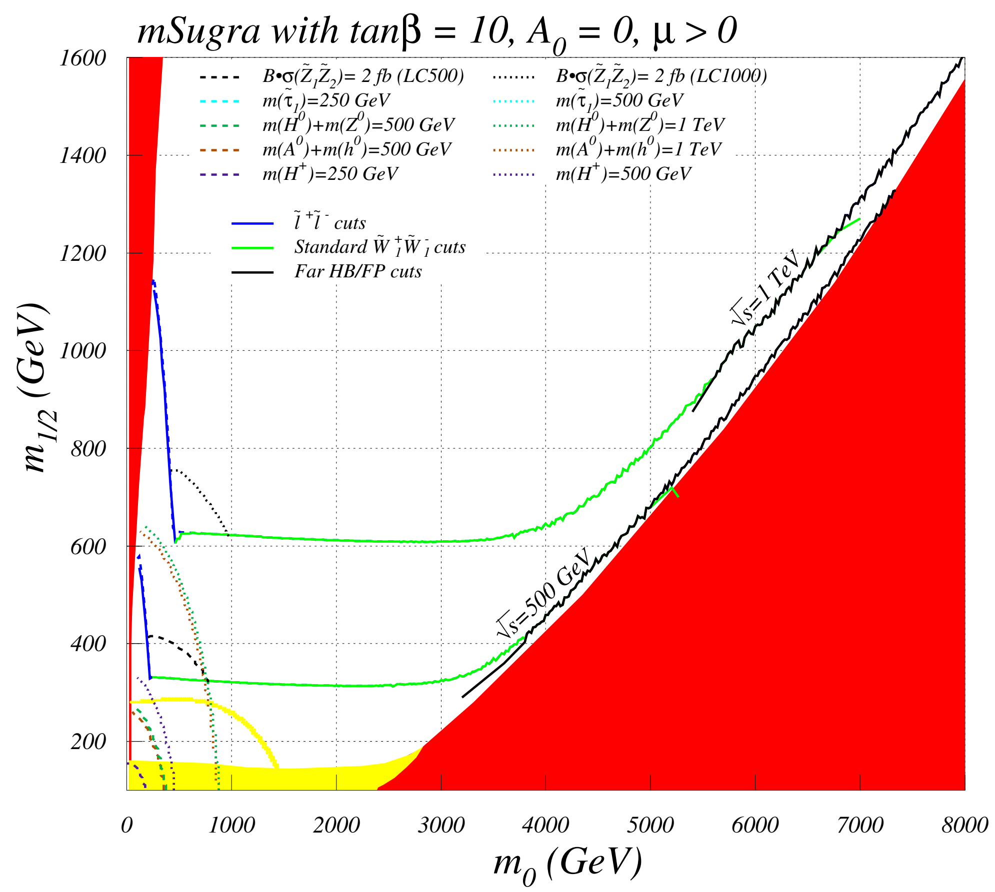

Figure 5: Reach of a linear collider for supersymmetry in the mSUGRA model for $\sqrt{s} = 500$ and $1000\,\mathrm{GeV}$, for $\tan\beta = 10$, $A_0 = 0$ and $\mu > 0$. The colors on the various regions and on the different contours are as in figure 1.

Finally, we show the kinematic limit for $e^+e^- \to ZH$ (green-dashed or dotted contours), $e^+e^- \to Ah$ (orange dashed or dotted contours) and $e^+e^- \to H^+H^-$ (purple dashed or dotted contours). The dashes are for $\sqrt{s} = 0.5\,\mathrm{TeV}$, while dotted are for $\sqrt{s} = 1\,\mathrm{TeV}$. For $\tan\beta = 30$, these contours always lie below the sparticle reach contours, so if heavier SUSY Higgs bosons are seen (at least in the channels mentioned above), sparticles should also be seen if SUSY is realized as in the mSUGRA framework.

In figure 5, we show LC reach contours for the same mSUGRA parameter plane as in figure 1, except this time $\tan\beta = 10$. Qualitatively, many of the reach contours are similar to the $\tan\beta = 30$ case of figure 1, and in particular, the new cuts designed to access the far HB/FP region again allow the LC reach to extend into the high $m_{1/2}$ section of the hyperbolic branch. One difference for $\tan\beta = 10$ results is that the $\tilde{\tau}_1^+\tilde{\tau}_1^-$ kinematic reach contour now lies nearly atop the selectron/smuon reach contour using the dilepton cuts described at the beginning of this section.

In figure 6, we show the same reach contours in the m_0 vs. $m_{1/2}$ plane, but this time for $\tan\beta = 45$ and $\mu < 0$. The standard slepton pair and chargino pair production reach contours are similar to the low $\tan\beta$ cases. In this case, the far HB/FP region cuts allow the

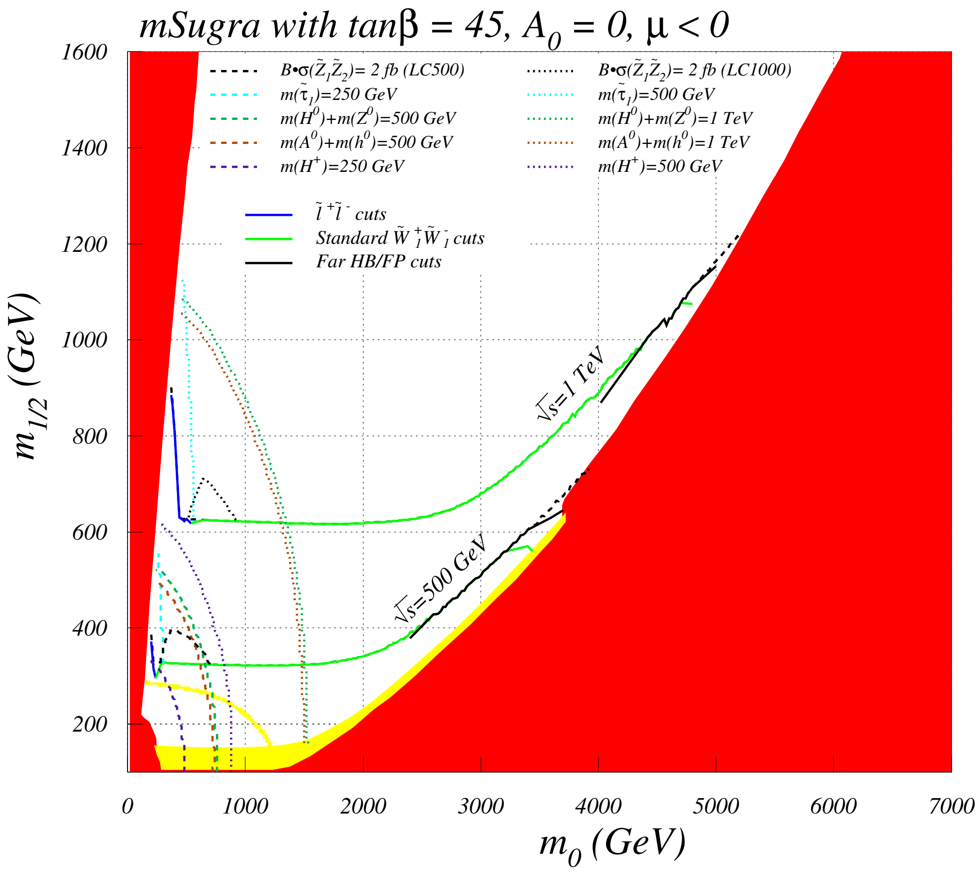

Figure 6: Reach of a linear collider for supersymmetry in the mSUGRA model for $\sqrt{s} = 500$ and 1000 GeV, for $\tan\beta = 45$, $A_0 = 0$ and $\mu < 0$. The colors on the various regions and on the different contours are as in figure 5.

reach to be extended, although the reach contour terminates in the part of the red region where the numerical solutions to the renormalization group equations do not converge as per the criteria in ISAJET. A tiny region remains inaccessible to our new cuts, between the black solid contours and the dashed contours that depicts the kinematic limit for chargino pair production. Another feature of the $\tan\beta = 45$ plot is that the stau pair kinematic region has expanded even more beyond where signals for $\tilde{e}_R$ and $\tilde{\mu}_R$ may be accessible in the dilepton channel. In addition, for this large value of $\tan\beta$, the heavy Higgs bosons are much lighter than the low $\tan\beta$ cases [38], and now there exist regions of parameter space where ZH and Ah production may be accessible, while sparticles are not: indeed such a situation would point to a large value of $\tan\beta$ which would of course be independently measureable from the properties of the detected Higgs bosons [39]. These regions all occur well below the reach of the LHC for SUSY, which will be shown in section 4. Thus, if nature chooses $\tan\beta = 45$ in an mSUGRA-like model, and the LC sees only Higgs bosons beyond the SM, it is likely that the existence of SUSY would already have been established by LHC experiments.

In figure 7, we show our final LC reach plot, taking $\tan\beta = 52$ with $\mu > 0$. In this case, there is still substantial reach for chargino pairs via the standard cuts, and the special

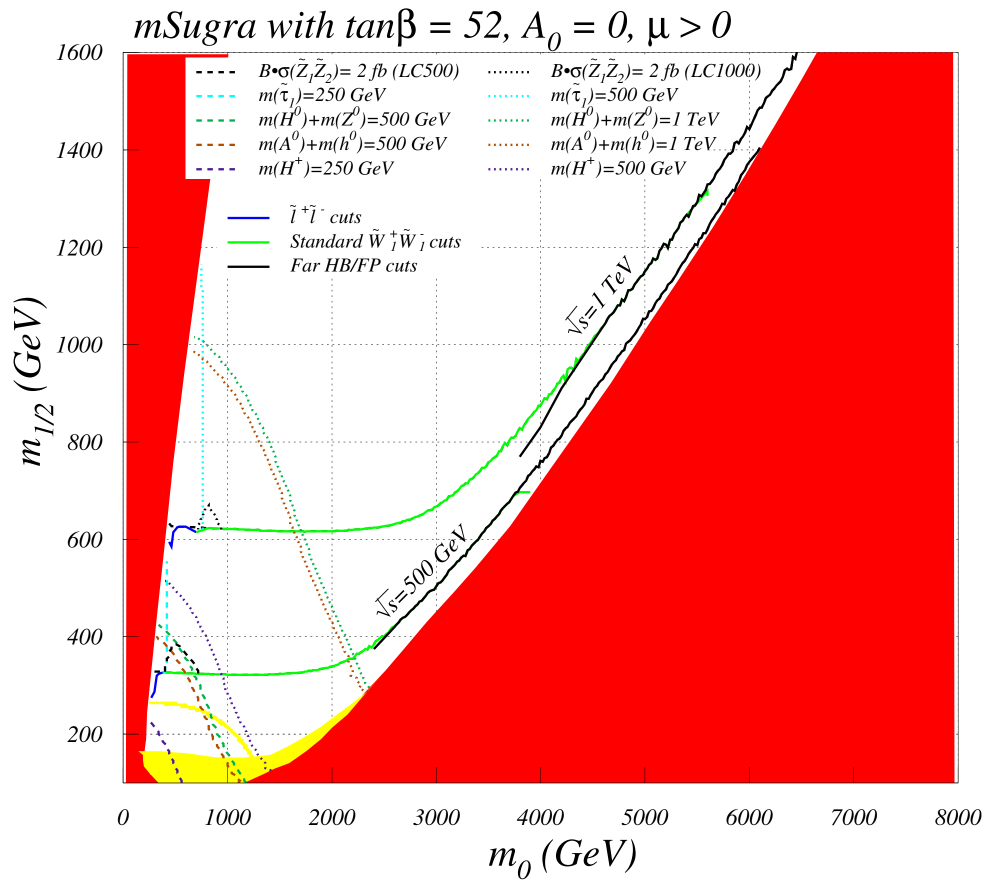

Figure 7: Reach of a linear collider for supersymmetry in the mSUGRA model for $\sqrt{s} = 500$ and 1000 GeV, for $\tan\beta = 52$, $A_0 = 0$ and $\mu > 0$. The colors on the various regions and on the different contours are as in figure 5.

cuts for the far HB/FP region again allow extended reach into this area. For this large a value of $\tan\beta$, the dilepton reach contour has been completely consumed by the expanding forbidden region on the left where $\tilde{\tau}_1$ becomes the LSP. In addition, the $e^+e^- \to \widetilde{Z}_1\widetilde{Z}_2$ reach region has shrunk due to the increased branching fraction for $\widetilde{Z}_2 \to \tilde{\tau}_1\tau$ decay. However, the kinematic reach for stau pairs has greatly increased, and becomes especially important for very large $\tan\beta$, especially if nature has chosen to reduce LSP dark matter from the early universe via co-annihilation with staus.

3. Comparison of LC reach with Tevatron, LHC and $\Omega_{\widetilde{Z}_1}h^2$

In this section, we present an overview of the reach of a LC in comparison to the reach for sparticles that can be obtained by the Fermilab Tevatron and the CERN LHC. In addition, we show regions of relic neutralino dark matter density in accord with the recent WMAP measurements.

Our first results are shown in figure 8 which shows the same parameter space plane as in figure 5. In this case, however, we plot the composite reach plot of a $\sqrt{s} = 0.5$ and 1 TeV LC for discovery of sparticles assuming 100 fb^{-1} of integrated luminosity. The LC reach plots now consist of combined 1.) slepton pair reach via dileptons (we also show the kinematically accesible stau pair production contour, if it is beyond the slepton reach), 2.) the chargino pair reach via $1\ell + 2j + \not{E}_T$ events, with either the standard cuts or the cuts specialized for searches in the HB/FP region, and 3.) the region of $\widetilde{Z}_1\widetilde{Z}_2 \to b\bar{b} + \not{E}_T$. In addition, we superimpose on this plot the reach of the Fermilab Tevatron for SUSY via the clean trilepton signal originating from $p\bar{p} \to \widetilde{W}_1\widetilde{Z}_2X \to 3\ell + \not{E}_T + X$, where X denotes assorted hadronic debris. The Tevatron reach was extended into the HB/FP region in ref. [26]; we show the optimistic reach assuming a 3σ signal with $25\,\mathrm{fb}^{-1}$ of integrated luminosity. In addition, we show the reach of the CERN LHC as derived in ref. [27], assuming $100\,\mathrm{fb}^{-1}$ of integrated luminosity. We have also added to the plot the green region, which denotes parameter space points with relic density $\Omega_{\widetilde{Z}_1}h^2 < 0.129$, as required by the recent WMAP measurements.[5] For our relic density calculation [40] we have evaluated all relevant neutralino annihilation and co-annihilation processes in the early universe using the CompHEP program. We have implemented relativistic thermal averaging of the annihilation cross section times velocity, which is useful to get the appropriate relic density in the vicinity of s-channel poles (where the annihilating neutralinos may have substantial velocities) using the formulae of Gondolo and Edsjö [41].

The dark matter allowed region splits into three distinct regions for $\tan\beta = 10$. On the far left of the plot at low m_0 is the stau co-annihilation region, which blends into the bulk annihilation region at low $m_{1/2}$ values. Note that the bulk region is largely below the LEP2 $m_h = 114.4\,\mathrm{GeV}$ contour. We also see that the stau co-annihilation region extends to $m_{1/2}$ values as high as $\sim 900\,\mathrm{GeV}$. For $\tan\beta = 10$, we see that a $\sqrt{s} = 0.5\,\mathrm{TeV}$ e^+e^- collider should be able to scan much of the stau co-annihilation region, while a $\sqrt{s} = 1\,\mathrm{TeV}$ machine can cover it entirely (as can the LHC). Another region of relic density is the small strip at constant $m_{1/2} \sim 100\,\mathrm{GeV}$, where neutralinos can annihilate through the narrow s-channel pole from the light Higgs boson h. This region can be covered by all the colliders, including the Fermilab Tevatron. Finally, adjacent to the REWSB excluded region at large m_0 is shown the dark matter allowed region in the HB/FP region, where the LSP has a significant higgsino component, which facilitates neutralino annihilation to WW and ZZ pairs in the early universe. The Fermilab Tevatron reach does not extend into this regime. The $\sqrt{s} = 0.5\,\mathrm{TeV}$ LC can explore the kinematically allowed portion of the lower HB/FP region (which is the region favored by the fine-tuning analysis of ref. [20]) via standard cuts and the cuts specialized to the far HB/FP region. The $\sqrt{s} = 1\,\mathrm{TeV}$ colider can explore *all* the HB/FP region which is dark matter allowed, until $m_{1/2}$ becomes greater than $\sim 900\,\mathrm{GeV}$. The portion of the HB/FP region with $m_{1/2} > 900\,\mathrm{GeV}$, while allowed by dark matter as well as other experimental constraints, becomes more difficult to reconcile with fine-tuning considerations. The new cuts proposed in section 2 allow the LC SUSY search region to extend well beyond the reach of the CERN LHC, which extends only to $m_{1/2} \sim 700\,\mathrm{GeV}$. The LHC reach is limited in the high $m_{1/2}$ part of the hyperbolic branch because sfermions and gluinos are too heavy to be produced at an appreciable rate. Chargino and neutralino pairs can still be produced at the LHC in the high $m_{1/2}$

[5]The WMAP allowed region including the lower bound would appear as a very narrow strip following the border of the green region.

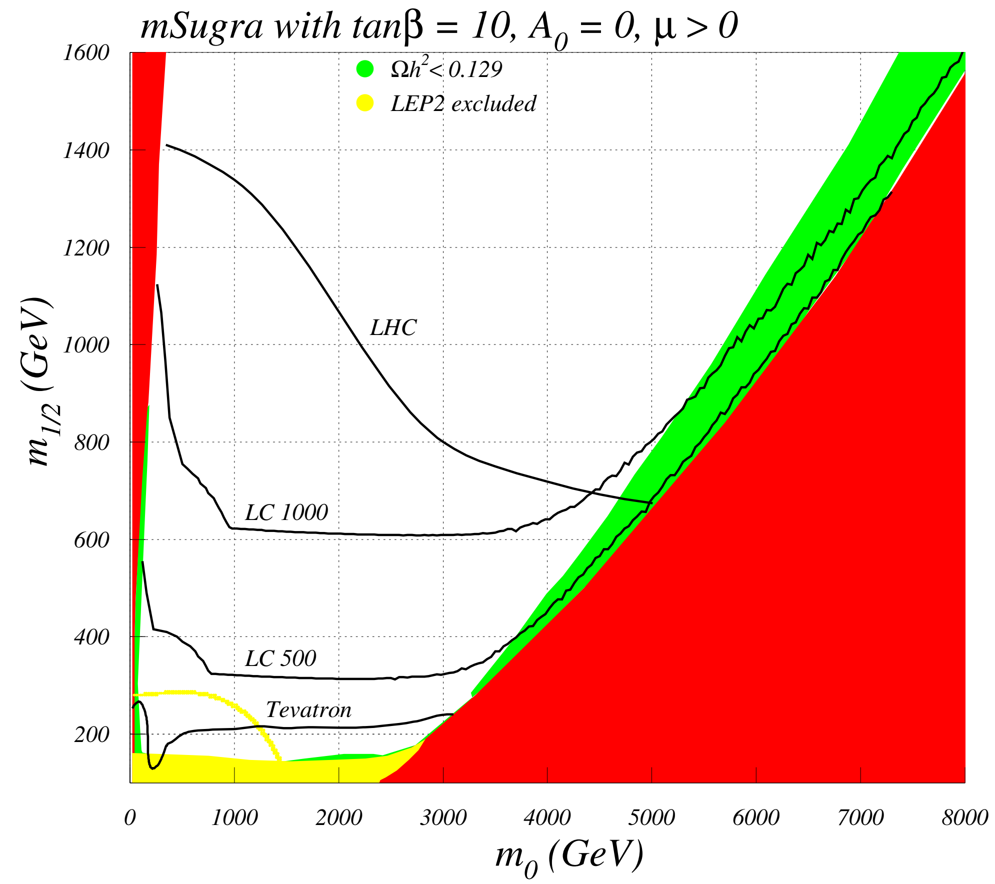

Figure 8: Reach of a $\sqrt{s} = 0.5$ and 1 TeV LC for sparticles in the mSUGRA model for $\tan\beta = 10$, $A_0 = 0$ and $\mu > 0$. We also show the reach of the Fermilab Tevatron assuming $10\,\mathrm{fb}^{-1}$ of integrated luminosity (for isolated trileptons) and the reach of the CERN LHC assuming $100\,\mathrm{fb}^{-1}$ of integrated luminosity. Finally, the green shaded region shows points where the relic density $\Omega_{\widetilde{Z}_1}h^2 < 0.129$ as dictated by WMAP.

part of the hyperbolic branch, but the soft visible energy emanating from chargino and neutralino decay makes detection above background very difficult. The high $m_{1/2}$ part of the hyperbolic branch yields a first example of a region of mSUGRA model parameter space where *sparticles can be discovered at a LC, whereas the CERN LHC reach for sparticles has petered out.* Moreover, this additional reach area comes in precisely at a very compelling dark matter allowed region of the mSUGRA model.

In figure 9, we show the same plot, except this time for $\tan\beta = 30$. Many features of the plot are qualitatively similar to the $\tan\beta = 10$ case. In this case, the stau co-annihilation corridor now extends up to $m_{1/2}$ values as high as 1050 GeV. The entire stau co-annihilation corridor can potentially be explored by a $\sqrt{s} = 1$ TeV LC, but only if a stau pair search is made in addition to the dilepton search. In this case, the Tevatron reach extends just to the tip of the dark matter allowed HB/FP region. The LHC reach in the HB/FP region is again limited to $m_{1/2} < 700$ GeV values, while the $\sqrt{s} = 0.5$ and especially the $\sqrt{s} = 1$ TeV LC can explore much of the HB/FP region, even for $m_{1/2}$ values far in excess of 700 GeV.

JHEP02(2004)007

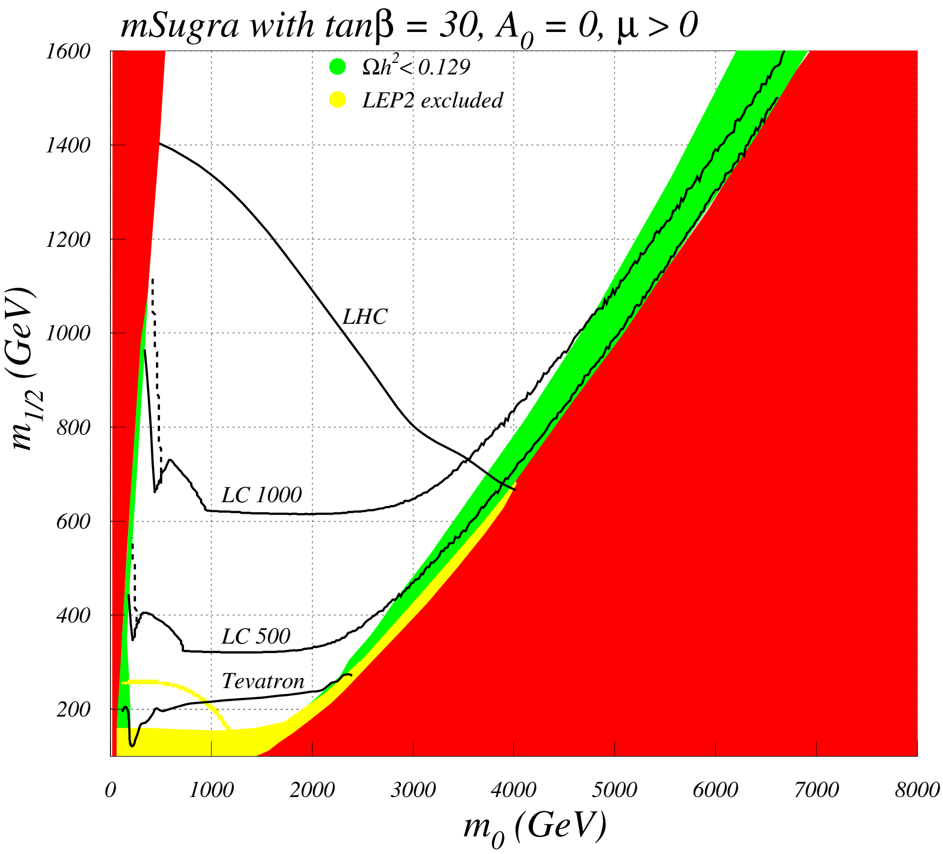

Figure 9: Reach of a $\sqrt{s} = 0.5$ and 1 TeV LC for sparticles in the mSUGRA model for $\tan\beta = 30$, $A_0 = 0$ and $\mu > 0$. We also show the reach of the Fermilab Tevatron assuming $10\,\mathrm{fb}^{-1}$ of integrated luminosity (for isolated trileptons) and the reach of the CERN LHC assuming $100\,\mathrm{fb}^{-1}$ of integrated luminosity. Finally, the green shaded region shows points where the relic density $\Omega_{\widetilde{Z}_1} h^2 < 0.129$ as dictated by WMAP. We denote the kinematic limit for stau pair production at LCs by a dashed black contour.

The dark matter relic density is qualitatively different for the case of $\tan\beta = 45$, $\mu < 0$ shown in figure 10. Here, a large new dark matter allowed region has emerged, namely the A-annihilation funnel which is characteristic of the mSUGRA model at very large $\tan\beta$. As $\tan\beta$ increases, the derived value of m_A decreases, until a region where $m_A \simeq 2m_{\widetilde{Z}_1}$ arises, where neutralinos can efficiently annihilate through the very broad A and also the H s-channel resonances. It can be seen from the figure that the A-annihilation funnel region extends well beyond the reach of both the $\sqrt{s} = 0.5$ and 1 TeV LC. In addition, the stau co-annihilation strip rises to $m_{1/2}$ values that are also beyond the reach of a 1 TeV LC. The CERN LHC can explore essentially all of the A-annihilation funnel for this particular value of $\tan\beta$ and sign of μ. Also, in this case, the $\sqrt{s} = 0.5$ TeV LC can explore the HB/FP region only up to $m_{1/2} \sim 600$ GeV where the $m_{\widetilde{W}_1} = 250$ GeV contour intersects the excluded region. The 1 TeV LC has a reach that extends again well beyond the limit of the LHC reach in the HB/FP region.

In figure 11, we show the $\tan\beta = 52$ mSUGRA plane for $\mu > 0$. In this case, the effect of the A-annihilation funnel is just beginning to enter the m_0 vs. $m_{1/2}$ plane from the left, so

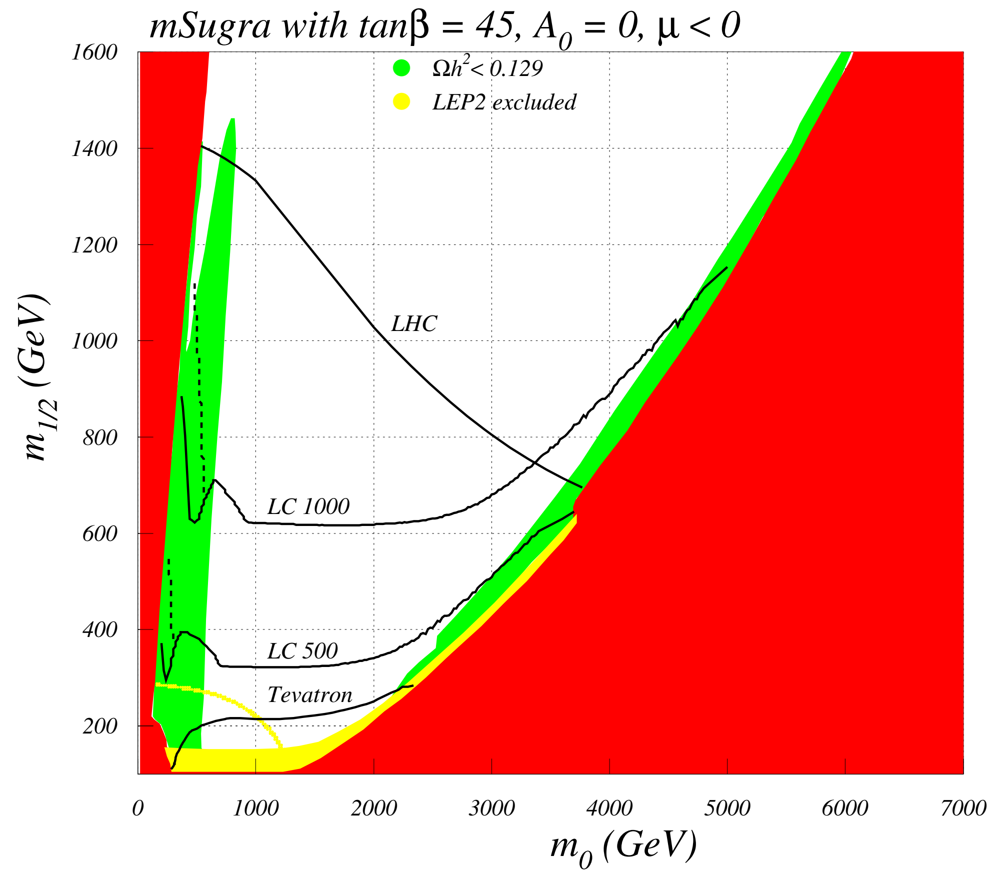

Figure 10: Reach of a $\sqrt{s} = 0.5$ and 1 TeV LC for sparticles in the mSUGRA model for $\tan\beta = 45$, $A_0 = 0$ and $\mu < 0$. We also show the reach of the Fermilab Tevatron assuming $10\,\mathrm{fb}^{-1}$ of integrated luminosity (for isolated trileptons) and the reach of the CERN LHC assuming $100\,\mathrm{fb}^{-1}$ of integrated luminosity. Finally, the green shaded region shows points where the relic density $\Omega_{\widetilde{Z}_1}h^2 < 0.129$ as dictated by WMAP. We denote the kinematic limit for stau pair production at LCs by a dashed black contour.

that points along the low m_0 forbidden region have a low relic density because neutralinos can annihilate via stau coannihilation, via t-channel slepton (mainly stau) exchange (low $m_{1/2}$) *and* partly due to annihilation through the s-channel A resonance. In this case, the A resonance corridor is actually off the plot, but since the A width is so large ($\Gamma_A \sim 25$ GeV for $m_{1/2} \sim 600$ GeV), the value of $2m_{\widetilde{Z}_1}$ can be a few partial widths away from resonance and still give significant contributions to the neutralino annihilation rate. For this large a $\tan\beta$ value, the stau co-annihilation strip reaches $m_{1/2}$ values far beyond the reach of LCs or even the LHC. In the HB/FP region, the new cuts presented in section 2 again give the LCs a reach well beyond the LHC for $m_{1/2} > 700$ GeV.

4. Determination of model parameters in the HB/FP region

Once a signal for supersymmetry is established at a LC, then the next task will be to scrutinize the signal to elucidate production and decay processes, extract sparticle masses, spins and other quantum numbers, and ultimately to determine parameters of the underly-

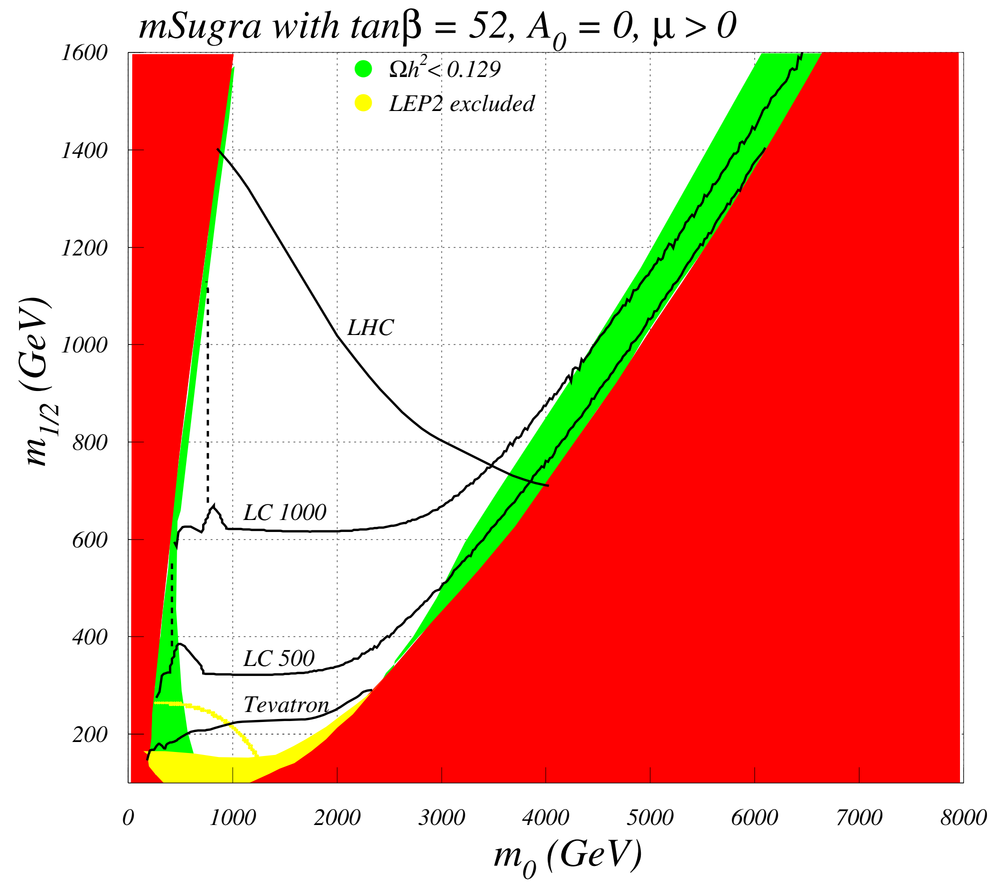

Figure 11: Reach of a $\sqrt{s} = 0.5$ and 1 TeV LC for sparticles in the mSUGRA model for $\tan\beta = 52$, $A_0 = 0$ and $\mu > 0$. We also show the reach of the Fermilab Tevatron assuming $10\,\mathrm{fb}^{-1}$ of integrated luminosity (for isolated trileptons) and the reach of the CERN LHC assuming $100\,\mathrm{fb}^{-1}$ of integrated luminosity. Finally, the green shaded region shows points where the relic density $\Omega_{\widetilde{Z}_1}h^2 < 0.129$ as dictated by WMAP. We denote the kinematic limit for stau pair production at LCs by a dashed black contour.

ing model. Many groups have examined different case studies [42]. In this section, we will examine a case study in the low $m_{1/2}$ part of the HB/FP region in an attempt to extract the underlying parameters of the MSSM, which may in turn point to nature actually being described by parameters in the HB/FP region.

Toward this end, we consider Case 2, with the mSUGRA parameters set given by

$$m_0 = 2500\,\mathrm{GeV}\,, \quad m_{1/2} = 300\,\mathrm{GeV}\,, \quad A_0 = 0\,, \quad \tan\beta = 30\,, \quad \mathrm{sign}(\mu) = +1\,.$$

Sample sparticle masses and parameters are given in table 3. For these parameter choices, $|\mu| < M_2$, so that the light chargino and lightest neutralino have significant higgsino components. The chargino mass $m_{\widetilde{W}_1} = 113.1\,\mathrm{GeV}$, and is just beyond the reach of LEP2. The LSP mass is $m_{\widetilde{Z}_1} = 85.6\,\mathrm{GeV}$, so that the mass gap $m_{\widetilde{W}_1} - m_{\widetilde{Z}_1} = 27.5\,\mathrm{GeV}$. The $\widetilde{W}_1$ decays via 3-body modes into $\widetilde{Z}_1 f\bar{f}'$, where f and f' are SM fermions. The decays are dominated by the W boson exchange graphs, so that decays $\widetilde{W}_1 \to \widetilde{Z}_1 f\bar{f}'$ have similar branching fractions to $W \to f\bar{f}'$ decays.

We begin by generating $e^+e^- \to$ all SUSY particles for the signal, and generate SM backgrounds using all ISAJET SM processes. We first require all events to pass the standard chargino pair cuts for $1\ell + 2j + \not{E}_T$ events as detailed at the beginning of section 2. Next, following case study 4 of ref. [29], we require missing mass $\not{m} > 240\,\mathrm{GeV}$. The resulting signal and also background events are plotted in figure 12 in the $E(jj)$ vs. $m(jj)$ plane. SUSY and Higgs boson events are denoted by black dots, while SM background events are denoted by red crosses. The chargino pair events populate the cluster at low $m(jj)$, since the dijet mass from chargino decay is bounded by the $\widetilde{W}_1 - \widetilde{Z}_1$ mass difference. If the chargino decays via $\widetilde{W}_1 \to W\widetilde{Z}_1 \to q\bar{q}'\widetilde{Z}_1$, we would expect that the $E(jj)$ distribution would have well-defined upper and lower endpoints that depend only on $m_{\widetilde{W}_1}$ and $m_{\widetilde{Z}_1}$ (and, of course M_W), as in case study 1 of ref. [31].

parameter	value (GeV)
M_2	236.5
M_1	122.0
μ	121.6
$m_{\tilde{g}}$	833.2
$m_{\tilde{u}_L}$	2548.1
$m_{\tilde{e}_L}$	2503.9
$m_{\widetilde{W}_1}$	113.1
$m_{\widetilde{W}_2}$	274.8
$m_{\widetilde{Z}_1}$	85.6
$m_{\widetilde{Z}_2}$	135.0
$m_{\widetilde{Z}_3}$	142.2
$m_{\widetilde{Z}_4}$	281.5
m_A	2129.4
m_h	118.8
$\Omega_{\widetilde{Z}_1}h^2$	0.0423
$BF(b \to s\gamma)$	3.84×10^{-4}
Δa_μ	2.3×10^{-10}

Table 3: Masses and parameters in GeV units for Case 2 for $m_0 = 2500\,\mathrm{GeV}$, $m_{1/2} = 300\,\mathrm{GeV}$, $A_0 = 0$, $\tan\beta = 30$, $\mathrm{sign}\,\mu = +1$ in the mSUGRA model. The spectra is obtained using ISAJET v7.69.

In the HB/FP region, the $\widetilde{W}_1 - \widetilde{Z}_1$ mass gap is small, and the decay to on-shell W is kinematically inaccessible. We can, however, adapt this strategy by forcing "two-body kinematics" on these events by first selecting events in narrow bins in $m(jj)$ and studying separately their $E(jj)$ distributions. This is done in figure 13, where we show the $E(jj)$ distribution for $m(jj)$ bins of width 4 GeV, centered at 8, 12, 16 and 20 GeV, corresponding to an integrated luminosity of $100\,\mathrm{fb}^{-1}$. This is the "data". The energy of the dijet cluster is bounded by

$$\gamma(E^*_{jj} - \beta p^*_{jj}) \leq E(jj) \leq \gamma(E^*_{jj} + \beta p^*_{jj})\,, \tag{4.1}$$

where $E^*_{jj} = (m^2_{\widetilde{W}_1} + m^2(jj) - m^2_{\widetilde{Z}_1})/2m_{\widetilde{W}_1}$, $p^*_{jj} = \sqrt{E^{*2}_{jj} - m^2(jj)}$, $\gamma = E_{\widetilde{W}_1}/m_{\widetilde{W}_1}$, $\beta = p^*_{jj}/E^*_{jj}$ and $E_{\widetilde{W}_1} = \sqrt{s}/2$, up to energy mismeasurement errors, jet clustering, particle losses, bremsstrahlung and finite width bins in $m(jj)$. The corresponding "theoretical predictions" shown by the smooth curve are obtained by generating a much larger sample of the same events and fitting this larger sample (corresponding to an integrated luminosity of $600\,\mathrm{fb}^{-1}$) to the function,

$$\begin{aligned} F(E, m_{\widetilde{W}_1}, m_{\widetilde{Z}_1}; A, B, C, D) \;=\; & N\left\{1 + \exp\left[\frac{E_{\min} + A - E}{B\sigma_{E_{\min}}}\right]\right\}^{-1} \times \\ & \times \left\{1 + \exp\left[\frac{-E_{\max} + C + E}{D\sigma_{E_{\max}}}\right]\right\}^{-1}, \end{aligned} \tag{4.2}$$

where $E_{\min}$ and $E_{\max}$ are calculated for each bin in $m(jj)$ taking the central $m(jj)$ value in that bin, and input values for $m_{\widetilde{W}_1}$ and $m_{\widetilde{Z}_1}$; $\sigma_{E_{\min}}$ ($\sigma_{E_{\max}}$) is the absolute value of

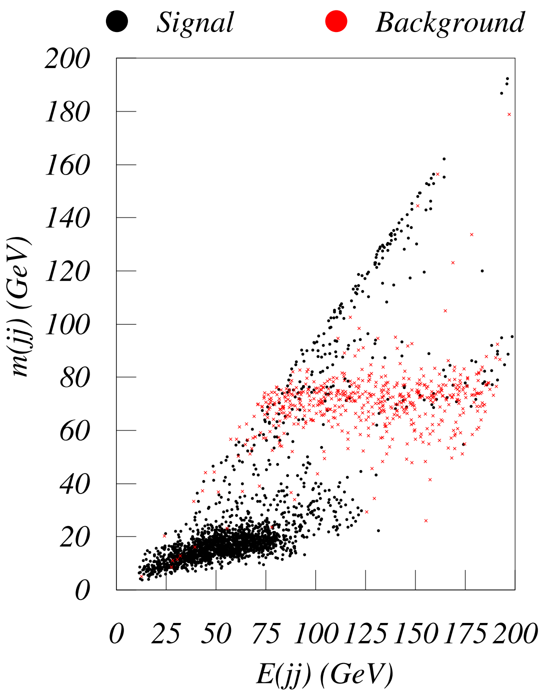

Figure 12: Scatter plot of SUSY signal events (black dots) and SM background (red x's) after standard cuts plus $\not{m} > 240$ GeV cuts, in the E_{jj} vs. $m(jj)$ plane. Chargino pair events occupy the low $m(jj)$ region.

the difference between $E_{\rm min}$ ($E_{\rm max}$) at the highest $m(jj)$ value in each $m(jj)$ bin and $E_{\rm min}$ ($E_{\rm max}$) for $m(jj)$ at the center of this bin. The small contribution from the SM background has also been included. The parameters A, B, C and D are separately determined for each bin in $m(jj)$ and serve to fit the shapes of the corresponding distributions, while N is adjusted to give the normalization near the maximum of E_{jj} distribution corresponding to an integrated luminosity of 100 fb^{-1}.

Next, we proceed to perform a χ^2 fit to obtain $m_{\widetilde{W}_1}$ and $m_{\widetilde{Z}_1}$ from our synthetic data sample, using the fitted function (4.2) for the theoretical prediction[6] for chargino and neutralino masses close to those for Case 2. In other words, for a grid of points in the $(m_{\widetilde{W}_1}, m_{\widetilde{Z}_1})$ plane, we evaluate,

$$\chi^2(m_{\widetilde{W}_1}, m_{\widetilde{Z}_1}) = \sum_{\rm bins}\sum_{E}\left(\frac{F(E, m_{\widetilde{W}_1}(inp), m_{\widetilde{Z}_1}(inp)) - F(E, m_{\widetilde{W}_1}, m_{\widetilde{Z}_1})}{\sqrt{F(E, m_{\widetilde{W}_1}, m_{\widetilde{Z}_1})}}\right)^2 \tag{4.3}$$

where $\sum_{\rm bins}$ means that we sum over all four bins in $m(jj)$, and $\sum_E$ denotes the summation over all bins in E_{jj} and find the values of chargino and neutralino masses for which this quantity is minimized. These best fit values, together with the regions where $\Delta\chi^2 \leq 2.3$ (68.3% CL) and ≤ 4.6 (90% CL) are shown in figure 14. We see that it is possible to determine $m_{\widetilde{W}_1}$ and $m_{\widetilde{Z}_1}$ at approximately the 10% level.

[6]Of course, the parameters $E_{\rm min}$, $\sigma_{E_{\rm min}}$, $E_{\rm max}$ and $\sigma_{E_{\rm max}}$ depend on $m_{\widetilde{W}_1}$ and $m_{\widetilde{Z}_1}$ via (4.1) and the equations following that. We assume that the parameters A, B, C and D do not change.

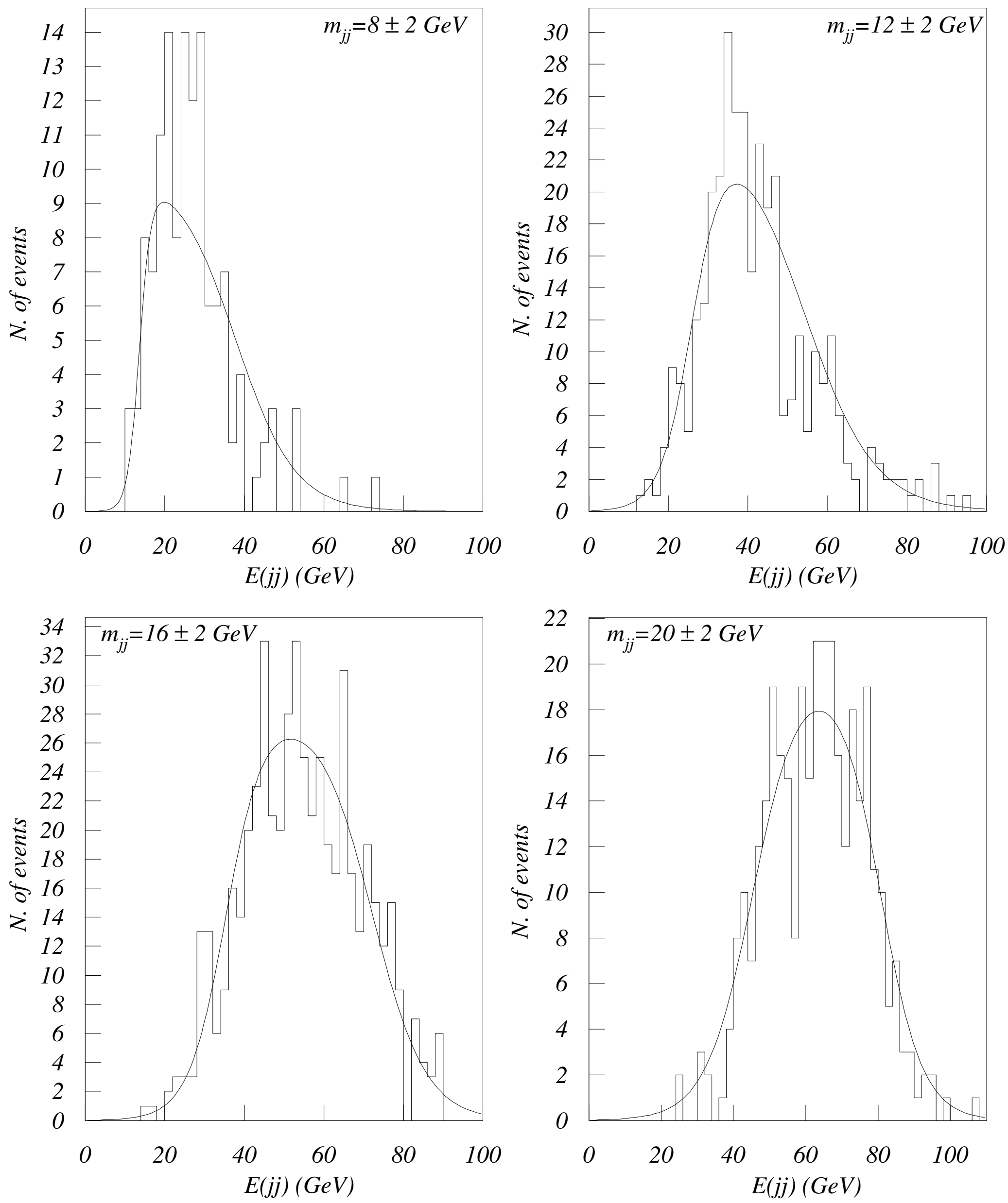

Figure 13: Distribution of E_{jj} for $\ell+2-jet$ events after standard cuts together with $\not{m} > 240\,\mathrm{GeV}$, with events restricted to narrow bins of $m(jj)$. The histograms show these distributions for the synthetic data sample while the solid line shows the corresponding theoretical expectation obtained as described in the text.

Having determined the values of $m_{\widetilde{W}_1}$ and $m_{\widetilde{Z}_1}$, the next step is to examine what we can say about the underlying MSSM parameters μ, M_2 and $\tan\beta$ that enter the chargino mass matrix. To determine three unknowns, we need to experimentally determine one more quantity which we take to be the cross section for $1\ell + 2j + \not{E}_T$ events from chargino pair production. Almost all the signal arises from chargino pair production if we require $m(jj) < 25\,\mathrm{GeV}$ and $E(jj) < 100\,\mathrm{GeV}$ as in figure 12. For $100\,\mathrm{fb}^{-1}$ of integrated luminosity, we find 1649 events, which translates to a measurement of $\sigma(e^+e^- \to \widetilde{W}_1^+\widetilde{W}_1^-) = 16.5{\pm}0.4\,\mathrm{fb}$ (after

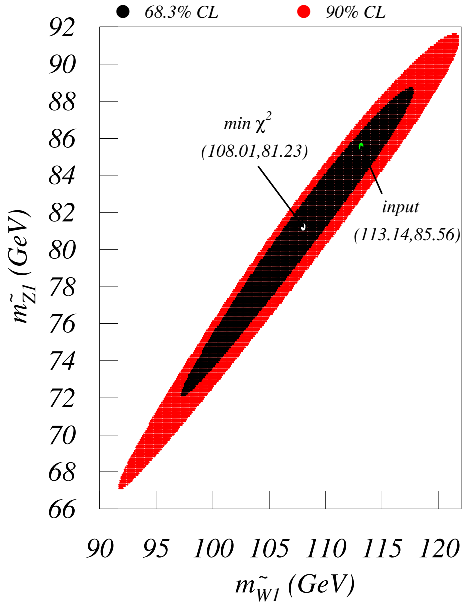

Figure 14: Fits to $m_{\widetilde{W}_1}$ and $m_{\widetilde{Z}_1}$ and the associated error ellipses for Case 2 in the text.

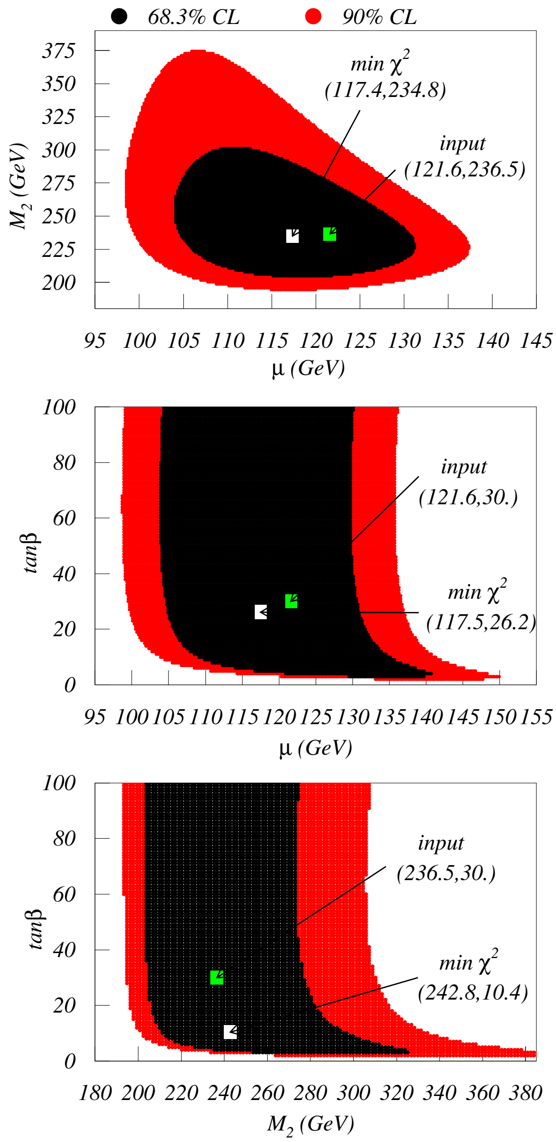

Figure 15: Fits to μ, M_2 and $\tan\beta$ from the measured values of $m_{\widetilde{W}_1}$, $m_{\widetilde{Z}_1}$ and $\sigma(\widetilde{W}_1^+\widetilde{W}_1^-)$, and the associated 68.3% and 90% CL regions for Case 2. The green squares denote the fitted values while the white squares show the corresponding input values of the parameters.

all the cuts), or 2.5% statistical error. Other systematic errors will be present, although these may be controllable by precision measurement of many SM processes. We perform a fit to the MSSM parameters using the values of $m_{\widetilde{W}_1}$, $m_{\widetilde{Z}_1}$ and $\sigma(\widetilde{W}_1^+\widetilde{W}_1^-)$ as determined above. We scan over MSSM model parameters, using 1-loop corrected mass relations for $m_{\widetilde{W}_1}$ and $m_{\widetilde{Z}_1}$ as given by ISAJET 7.69. In figure 15, we show the regions of a) the μ vs. M_2 plane, b) the μ vs. $\tan\beta$ plane and c) the M_2 vs. $\tan\beta$ plane that are allowed at the 68.3% and 90% CL. In each case, we have held the parameter not shown in the plane fixed at its input value. The result in frame (a) clearly shows that indeed $|\mu| \ll M_2$, providing strong support that the model parameters lie in the HB/FP region, and that the LSP has a significant higgsino component, enhancing the neutralino pair annihilation in the early universe.[7] While μ and M_2 can be well determined (at least for this case study), it is also evident from the figure that a precise determination of $\tan\beta$ is not possible in this case. This may not be so surprising, since in the HB/FP region, SUSY scalar masses that depend on Yukawa couplings and hence $\tan\beta$ are so heavy that they essentially decouple from observable physics, and the region is relatively invariant under changes in $\tan\beta$.

5. Summary and conclusions

The recent constraint on the relic density of neutralinos obtained from WMAP measurements, together with earlier determinations of $BF(b \to s\gamma)$ and $(g-2)_\mu$ select out regions of parameter space of the mSUGRA model. In the stau co-annihilation region, the H, A-annihilation funnel and in the HB/FP regions, very high values of m_0 and $m_{1/2}$ consistent with all constraints are possible: moreover, the so-called bulk region where sparticles are light is disfavored. These considerations motivated us to re-assess the reach of various collider and non-accelerator search experiments for supersymmetry. In this paper, we re-evaluate the reach of a $\sqrt{s} = 0.5$ and 1 TeV linear e^+e^- collider for SUSY in the context of the mSUGRA model, examining for the first time the reach in the HB/FP region. We find that a $\sqrt{s} = 1$ TeV LC can explore most of the stau co-annihilation region if $\tan\beta \lesssim 30$, although along with a dilepton search, a ditau search will also be needed. The H, A-annihilation funnel typically extends beyond the maximum reach of a LC. In the HB/FP region, chargino pairs may be kinematically accessible to a LC, but the energy release in chargino pairs can be small, reducing detection efficiency. Nonetheless, LCs should be able to probe much of the lower HB/FP region with standard chargino searches. In the upper HB/FP region, new cuts are proposed to allow signals from much of the small $\widetilde{W}_1 - \widetilde{Z}_1$ mass gap region to be observable above SM backgrounds. In this region, the reach of even a 500 GeV LC can exceed that of the CERN LHC! This is all the more important in that it occurs in a region of model parameter space which is allowed by all constraints, including those imposed by WMAP.

One should also stress that the LCs reach is also complimentary to reach of direct dark matter search experiments (DDMS) even though both kinds of experiments similarly cover much of the HB/FP region [28]. The complementarity of a LC occurs for the region which is very close to the no REWSB border. In this region, the neutralino relic density is so low that DDMS experiments are not able to cover this part of the parameter space even though the higgsino component of neutralino is significant. This region can be probed by experiments at a LC.

If a supersymmetric signal is found, then the next obvious step will be to determine the underlying MSSM parameters. We have performed a case study in the low $m_{1/2}$ part of the hyperbolic branch. In this region, we show that a measurement of $m_{\widetilde{W}_1}$ and $m_{\widetilde{Z}_1}$ is

[7] That $|\mu|$ is small can presumably also be determined by studying chargino production using polarized beams. Note that our determination does not require this capability.

possible at the 10% level. A measurement of the total chargino pair cross section to 2.5% allows a determination of MSSM parameters M_2 and μ, although $\tan\beta$ is more difficult to pin down. The resulting determination of M_2 and μ would point to a model with higgsino-like charginos and neutralinos. Together with absence (or low levels) of squark signals at the LHC, and the agreement of the chargino cross section with the expected s-channel contribution (pointing to heavy sneutrinos) these measurements would be indicative of an mSUGRA-type model in the HB/FP region. In case parameters are in the upper part of the hyperbolic branch, LC event characteristics may be sufficient at least to establish the production of massive particles, with associated decay products that are quite soft. An examination of how one would obtain information about the underlying scenario would be worthy of exploration.

Acknowledgments

This research was supported in part by the U.S. Department of Energy under contracts number DE-FG02-97ER41022 and DE-FG03-94ER40833.

References

[1] H. Baer, C. Balazs, A. Belyaev, J. Mizukoshi, X. Tata and Y. Wang, *Updated constraints on the minimal supergravity model*, *J. High Energy Phys.* **07** (2002) 050 [hep-ph/0205325]; *Updated constraints on the minimal supergravity model*, hep-ph/0210441;
For a review, see G. Eigen, R. Gaitskell, G.D. Kribs and K.T. Matchev, *Indirect investigations of supersymmetry*, *eConf* **C010630** (2001) P342 [hep-ph/0112312].

[2] ALEPH collaboration, R. Barate et al., *A measurement of the inclusive $b \to s\gamma$ branching ratio*, *Phys. Lett.* **B 429** (1998) 169;
CLEO collaboration, D. Cronin-Hennessy et al., *Hadronic mass moments in inclusive semileptonic B meson decays*, *Phys. Rev. Lett.* **87** (2001) 251808 [hep-ex/0108033];
Belle collaboration, K. Abe et al., *A measurement of the branching fraction for the inclusive $B \to X_s\gamma$ decays with Belle*, *Phys. Lett.* **B 511** (2001) 151 [hep-ex/0103042];
Theoretical results for $BF(b \to s\gamma)$ in the SM are contained in e.g. P. Gambino and M. Misiak, *Quark mass effects in $\bar{B} \to X_s\gamma$*, *Nucl. Phys.* **B 611** (2001) 338 [hep-ph/0104034];
Supersymmetric contributions are shown in e.g. H. Baer and M. Brhlik, *QCD improved $b \to s\gamma$ constraints on the minimal supergravity model*, *Phys. Rev.* **D 55** (1997) 3201 [hep-ph/9610224];
H. Baer, M. Brhlik, D. Castano and X. Tata, *$b \to s\gamma$ constraints on the minimal supergravity model with large* $\tan\beta$, *Phys. Rev.* **D 58** (1998) 015007 [hep-ph/9712305].

[3] Muon g-2 collaboration, G.W. Bennett et al., *Measurement of the positive muon anomalous magnetic moment to 0.7 ppm*, *Phys. Rev. Lett.* **89** (2002) 101804 [hep-ex/0208001];
A recent theoretical evaluation is given in M. Davier, S. Eidelman, A. Hocker and Z. Zhang, *Updated estimate of the muon magnetic moment using revised results from e^+e^- annihilation*, *Eur. Phys. J.* **C 31** (2003) 503 [hep-ph/0308213];
A survey of contributions from supersymmetric models can be found in H. Baer, C. Balazs, J. Ferrandis and X. Tata, *Impact of muon anomalous magnetic moment on supersymmetric models*, *Phys. Rev.* **D 64** (2001) 035004 [hep-ph/0103280].

[4] D.N. Spergel et al., *First year Wilkinson microwave anisotropy probe (WMAP) observations: determination of cosmological parameters*, *Astrophys. J. Suppl.* **148** (2003) 175 [astro-ph/0302209].

[5] For a review of WMAP implications for supersymmetric models, see A. Lahanas, N.E. Mavromatos and D.V. Nanopoulos, *WMAPing the universe: supersymmetry, dark matter, dark energy, proton decay and collider physics*, *Int. J. Mod. Phys.* **D 12** (2003) 1529 [hep-ph/0308251].

[6] A.H. Chamseddine, R. Arnowitt and P. Nath, *Locally supersymmetric grand unification*, *Phys. Rev. Lett.* **49** (1982) 970;
R. Barbieri, S. Ferrara and C.A. Savoy, *Gauge models with spontaneously broken local supersymmetry*, *Phys. Lett.* **B 119** (1982) 343;
N. Ohta, *Grand unified theories based on local supersymmetry*, *Prog. Theor. Phys.* **70** (1983) 542;
L.J. Hall, J. Lykken and S. Weinberg, *Supergravity as the messenger of supersymmetry breaking*, *Phys. Rev.* **D 27** (1983) 2359;
For reviews see, H.P. Nilles, *Supersymmetry, supergravity and particle physics*, *Phys. Rept.* **110** (1984) 1;
P. Nath, *Twenty years of SUGRA*, hep-ph/0307123.

[7] H. Goldberg, *Constraint on the photino mass from cosmology*, *Phys. Rev. Lett.* **50** (1983) 1419;
J.R. Ellis, J.S. Hagelin, D.V. Nanopoulos, K.A. Olive and M. Srednicki, *Supersymmetric relics from the big bang*, *Nucl. Phys.* **B 238** (1984) 453.

[8] G. Jungman, M. Kamionkowski and K. Griest, *Supersymmetric dark matter*, *Phys. Rept.* **267** (1996) 195 [hep-ph/9506380].

[9] H. Baer and M. Brhlik, *Cosmological relic density from minimal supergravity with implications for collider physics*, *Phys. Rev.* **D 53** (1996) 597 [hep-ph/9508321].

[10] J.R. Ellis, T. Falk, G. Ganis, K.A. Olive and M. Srednicki, *The CMSSM parameter space at large* $\tan\beta$, *Phys. Lett.* **B 510** (2001) 236 [hep-ph/0102098].

[11] G.W. Anderson and D.J. Castano, *Naturalness and superpartner masses or when to give up on weak scale supersymmetry*, *Phys. Rev.* **D 52** (1995) 1693 [hep-ph/9412322]; *Measures of fine tuning*, *Phys. Lett.* **B 347** (1995) 300 [hep-ph/9409419].

[12] ALEPH, DELPHI, L3 and OPAL collaborations, R. Barate et al., *Search for the standard model Higgs boson at LEP*, *Phys. Lett.* **B 565** (2003) 61 [hep-ex/0306033].

[13] M. Davier, S. Eidelman, A. Hocker and Z. Zhang, *Updated estimate of the muon magnetic moment using revised results from* e^+e^- *annihilation*, *Eur. Phys. J.* **C 31** (2003) 503 [hep-ph/0308213].

[14] J.R. Ellis, K.A. Olive, Y. Santoso and V.C. Spanos, *Supersymmetric dark matter in light of wmap*, *Phys. Lett.* **B 565** (2003) 176 [hep-ph/0303043];
U. Chattopadhyay, A. Corsetti and P. Nath, *Wmap constraints, SUSY dark matter and implications for the direct detection of SUSY*, *Phys. Rev.* **D 68** (2003) 035005 [hep-ph/0303201];
A.B. Lahanas and D.V. Nanopoulos, *Wmaping out supersymmetric dark matter and phenomenology*, *Phys. Lett.* **B 568** (2003) 55 [hep-ph/0303130].

[15] H. Baer and C. Balázs, *χ^2 analysis of the minimal supergravity model including WMAP, $g_\mu - 2$ and $b \to s\gamma$ constraints*, *JCAP* **05** (2003) 006 [hep-ph/0303114].

[16] J.R. Ellis, K.A. Olive, Y. Santoso and V.C. Spanos, *Likelihood analysis of the cmssm parameter space*, hep-ph/0310356.

[17] J.R. Ellis, T. Falk and K.A. Olive, *Neutralino stau coannihilation and the cosmological upper limit on the mass of the lightest supersymmetric particle*, *Phys. Lett.* **B 444** (1998) 367 [hep-ph/9810360];
J. Ellis, T. Falk, K. Olive and M. Srednicki, *Calculations of neutralino-stau coannihilation channels and the cosmologically relevant region of MSSM parameter space*, *Astropart. Phys.* **13** (2000) 181 [hep-ph/9905481], erratum *ibid.* **15** (2001) 413.

[18] M. Drees and M.M. Nojiri, *The neutralino relic density in minimal $N = 1$ supergravity*, *Phys. Rev.* **D 47** (1993) 376 [hep-ph/9207234];
H. Baer and M. Brhlik, *Neutralino dark matter in minimal supergravity: direct detection vs. collider searches*, *Phys. Rev.* **D 57** (1998) 567 [hep-ph/9706509];
H. Baer, M. Brhlik, M. Diaz, J. Ferrandis, P. Mercadante, P. Quintana and X. Tata, *Yukawa unified supersymmetric* SO(10) *model: cosmology, rare decays and collider searches*, *Phys. Rev.* **D 63** (2001) 015007 [hep-ph/0005027];
A. Djouadi, M. Drees and J.L. Kneur, *Constraints on the minimal supergravity model and prospects for SUSY particle production at future linear e^+e^- colliders*, *J. High Energy Phys.* **08** (2001) 055 [hep-ph/0107316];
J.R. Ellis, T. Falk, G. Ganis, K.A. Olive and M. Srednicki, *The cmssm parameter space at large* $\tan\beta$, *Phys. Lett.* **B 510** (2001) 236 [hep-ph/0102098];
L. Roszkowski, R. Ruiz de Austri and T. Nihei, *New cosmological and experimental constraints on the CMSSM*, *J. High Energy Phys.* **08** (2001) 024 [hep-ph/0106334];
A.B. Lahanas and V.C. Spanos, *Implications of the pseudo-scalar Higgs boson in determining the neutralino dark matter*, *Eur. Phys. J.* **C 23** (2002) 185 [hep-ph/0106345].

[19] K.L. Chan, U. Chattopadhyay and P. Nath, *Naturalness, weak scale supersymmetry and the prospect for the observation of supersymmetry at the Tevatron and at the LHC*, *Phys. Rev.* **D 58** (1998) 096004 [hep-ph/9710473].

[20] J.L. Feng, K.T. Matchev and T. Moroi, *Multi-tev scalars are natural in minimal supergravity*, *Phys. Rev. Lett.* **84** (2000) 2322 [hep-ph/9908309]; *Focus points and naturalness in supersymmetry*, *Phys. Rev.* **D 61** (2000) 075005 [hep-ph/9909334].

[21] H. Baer, C.-h. Chen, F. Paige and X. Tata, *Signals for minimal supergravity at the CERN large hadron collider: multi-jet plus missing energy channel*, *Phys. Rev.* **D 52** (1995) 2746 [hep-ph/9503271]; *Signals for minimal supergravity at the cern large hadron collider II. Multilepton channels*, *Phys. Rev.* **D 53** (1996) 6241 [hep-ph/9512383].

[22] H. Baer and M. Brhlik, *Neutralino dark matter in minimal supergravity: direct detection vs. collider searches*, *Phys. Rev.* **D 57** (1998) 567 [hep-ph/9706509].

[23] J.L. Feng, K.T. Matchev and F. Wilczek, *Neutralino dark matter in focus point supersymmetry*, *Phys. Lett.* **B 482** (2000) 388 [hep-ph/0004043]; *Prospects for indirect detection of neutralino dark matter*, *Phys. Rev.* **D 63** (2001) 045024 [astro-ph/0008115].

[24] W. de Boer, M. Herold, C. Sander and V. Zhukov, *Indirect evidence for the supersymmetric nature of dark matter from the combined data on galactic positrons, antiprotons and gamma rays*, hep-ph/0309029.

JHEP02(2004)007

[25] H. Baer, T. Krupovnickas and X. Tata, *Reach of the Fermilab Tevatron for minimal supergravity in the region of large scalar masses*, *J. High Energy Phys.* **07** (2003) 020 [hep-ph/0305325].

[26] H. Baer, T. Krupovnickas and X. Tata, *Reach of the Fermilab Tevatron for minimal supergravity in the region of large scalar masses*, *J. High Energy Phys.* **07** (2003) 020 [hep-ph/0305325];
See also H. Baer, M. Drees, F. Paige, P. Quintana and X. Tata, *Trilepton signal for supersymmetry at the fermilab Tevatron revisited*, *Phys. Rev.* **D 61** (2000) 095007 [hep-ph/9906233];
V.D. Barger and C. Kao, *Trilepton signature of minimal supergravity at the upgraded Tevatron*, *Phys. Rev.* **D 60** (1999) 115015 [hep-ph/9811489];
K.T. Matchev and D.M. Pierce, *New backgrounds in trilepton, dilepton and dilepton plus tau jet SUSY signals at the Tevatron*, *Phys. Lett.* **B 467** (1999) 225 [hep-ph/9907505].

[27] H. Baer, C. Balazs, A. Belyaev, T. Krupovnickas and X. Tata, *Updated reach of the CERN LHC and constraints from relic density, $b \to s\gamma$ and a_μ in the mSUGRA model*, *J. High Energy Phys.* **06** (2003) 054 [hep-ph/0304303];
For earlier work, see H. Baer, C.-H. Chen, F. Paige and X. Tata, *Signals for minimal supergravity at the CERN large hadron collider: multi-jet plus missing energy channel*, *Phys. Rev.* **D 52** (1995) 2746 [hep-ph/9503271];
H. Baer, C.-H. Chen, F. Paige and X. Tata, *Signals for minimal supergravity at the CERN large hadron collider II. Multilepton channels*, *Phys. Rev.* **D 53** (1996) 6241 [hep-ph/9512383];
H. Baer, C.-h. Chen, M. Drees, F. Paige and X. Tata, *Probing minimal supergravity at the CERN LHC for large* $\tan\beta$, *Phys. Rev.* **D 59** (1999) 055014 [hep-ph/9809223];
S. Abdullin and F. Charles, *Search for SUSY in (leptons +) jets + E_T^{miss} final states*, *Nucl. Phys.* **B 547** (1999) 60 [hep-ph/9811402];
CMS collaboration, S. Abdullin et al., *Discovery potential for supersymmetry in CMS*, *J. Phys.* **G 28** (2002) 469 [hep-ph/9806366];
B.C. Allanach, J.P.J. Hetherington, M.A. Parker and B.R. Webber, *Naturalness reach of the large hadron collider in minimal supergravity*, *J. High Energy Phys.* **08** (2000) 017 [hep-ph/0005186].

[28] H. Baer, C. Balazs, A. Belyaev and J. O'Farrill, *Direct detection of dark matter in supersymmetric models*, *JCAP* **09** (2003) 007 [hep-ph/0305191];
See also V.A. Bednyakov, H.V. Klapdor-Kleingrothaus and S. Kovalenko, *On SUSY dark matter detection with spinless nuclei*, *Phys. Rev.* **D 50** (1994) 7128 [hep-ph/9401262];
E. Diehl, G.L. Kane, C.F. Kolda and J.D. Wells, *Theory, phenomenology and prospects for detection of supersymmetric dark matter*, *Phys. Rev.* **D 52** (1995) 4223 [hep-ph/9502399];
R. Arnowitt and P. Nath, *Predictions of neutralino dark matter event rates in minimal supergravity unification*, *Phys. Rev.* **D 54** (1996) 2374 [hep-ph/9509260];
H. Baer and M. Brhlik, *Neutralino dark matter in minimal supergravity: direct detection vs. collider searches*, *Phys. Rev.* **D 57** (1998) 567 [hep-ph/9706509];
M. Drees, M.M. Nojiri, D.P. Roy and Y. Yamada, *Light higgsino dark matter*, *Phys. Rev.* **D 56** (1997) 276 [hep-ph/9701219];
A. Bottino, F. Donato, N. Fornengo and S. Scopel, *Probing the supersymmetric parameter space by wimp direct detection*, *Phys. Rev.* **D 63** (2001) 125003 [hep-ph/0010203];
J.R. Ellis, A. Ferstl and K.A. Olive, *Exploration of elastic scattering rates for supersymmetric dark matter*, *Phys. Rev.* **D 63** (2001) 065016 [hep-ph/0007113];

E. Accomando, R. Arnowitt, B. Dutta and Y. Santoso, *Neutralino proton cross sections in supergravity models*, *Nucl. Phys.* **B 585** (2000) 124 [hep-ph/0001019];
M.E. Gomez and J.D. Vergados, *Cold dark matter detection in SUSY models at large* $\tan\beta$, *Phys. Lett.* **B 512** (2001) 252 [hep-ph/0012020];
A.B. Lahanas, D.V. Nanopoulos and V.C. Spanos, *Dark matter direct searches and the anomalous magnetic moment of muon*, *Phys. Lett.* **B 518** (2001) 94 [hep-ph/0107151];
E.A. Baltz and P. Gondolo, *Implications of muon anomalous magnetic moment for supersymmetric dark matter*, *Phys. Rev. Lett.* **86** (2001) 5004 [hep-ph/0102147];
Y.G. Kim, T. Nihei, L. Roszkowski and R. Ruiz de Austri, *Upper and lower limits on neutralino wimp mass and spin-independent scattering cross section and impact of new* $(g-2)_\mu$ *measurement*, *J. High Energy Phys.* **12** (2002) 034 [hep-ph/0208069];
For a recent review and further references, see the review by C. Muñoz, *Dark matter detection in the light of recent experimental results*, hep-ph/0309346.

[29] H. Baer, R. Munroe and X. Tata, *Supersymmetry studies at future linear* e^+e^- *colliders*, *Phys. Rev.* **D 54** (1996) 6735 [hep-ph/9606325].

[30] A. Djouadi, M. Drees and J.L. Kneur, *Constraints on the minimal supergravity model and prospects for SUSY particle production at future linear* e^+e^- *colliders*, *J. High Energy Phys.* **08** (2001) 055 [hep-ph/0107316];
See also R. Arnowitt, B. Dutta, T. Kamon and V. Khotilovich, *mSUGRA at a 500 GeV linear collider*, hep-ph/0308159.

[31] T. Tsukamoto, K. Fujii, H. Murayama, M. Yamaguchi and Y. Okada, *Precision study of supersymmetry at future linear* e^+e^- *colliders*, *Phys. Rev.* **D 51** (1995) 3153;
See also *JLC-1, KEK Report 92-16* (1992).

[32] F.E. Paige, S.D. Protopescu, H. Baer and X. Tata, *Isajet 7.69: a Monte Carlo event generator for PP,* $\bar{p}p$ *and* e^+e^- *reactions*, hep-ph/0312045.

[33] P. Chen, *Differential luminosity under multi-photon beamstrahlung*, *Phys. Rev.* **D 46** (1992) 1186.

[34] This region appears in H. Baer, C.-H. Chen, R. Munroe, F.E. Paige and X. Tata, *Multichannel search for minimal supergravity at* $p\bar{p}$ *and* e^+e^- *colliders*, *Phys. Rev.* **D 51** (1995) 1046 [hep-ph/9408265];
Co-annihilation calculations may be found in C. Boehm, A. Djouadi and M. Drees, *Light scalar top quarks and supersymmetric dark matter*, *Phys. Rev.* **D 62** (2000) 035012 [hep-ph/9911496];
J. Ellis, K. Olive and Y. Santoso, *Calculations of neutralino stop coannihilation in the CMSSM*, *Astropart. Phys.* **18** (2003) 395 [hep-ph/0112113];
J. Edsjö, M. Schelke, P. Ullio and P. Gondolo, *Accurate relic densities with neutralino, chargino and sfermion coannihilations in mSUGRA*, *JCAP* **04** (2003) 001 [hep-ph/0301106].

[35] M. Drees, C.S. Kim and X. Tata, *Supersymmetry phenomenology and the nature of the lightest supersymmetric particle*, *Phys. Rev.* **D 37** (1988) 784.

[36] T. Sjostrand et al., *High-energy physics event generation with Pythia 6.1*, *Comput. Phys. Commun.* **135** (2001) 238 [hep-ph/0010017].

[37] A. Pukhov et al., *CompHEP: a package for evaluation of Feynman diagrams and integration over multi-particle phase space. User's manual for version 33*, hep-ph/9908288.

JHEP02(2004)007

[38] H. Baer, C.-H. Chen, M. Drees, F. Paige and X. Tata, *Collider phenomenology for supersymmetry with large* $\tan\beta$, *Phys. Rev. Lett.* **79** (1997) 986 [hep-ph/9704457].

[39] V.D. Barger, T. Han and J. Jiang, $\tan\beta$ *determination from heavy Higgs boson production at linear colliders*, *Phys. Rev.* **D 63** (2001) 075002 [hep-ph/0006223].

[40] H. Baer, C. Balazs and A. Belyaev, *Neutralino relic density in minimal supergravity with co-annihilations*, *J. High Energy Phys.* **03** (2002) 042 [hep-ph/0202076].

[41] J. Edsjö and P. Gondolo, *Neutralino relic density including coannihilations*, *Phys. Rev.* **D 56** (1997) 1879 [hep-ph/9704361];
This is based on earlier work by G.B. Gelmini, P. Gondolo and E. Roulet, *Neutralino dark matter searches*, *Nucl. Phys.* **B 351** (1991) 623.

[42] See ref. [31, 29] and also M.M. Nojiri, K. Fujii and T. Tsukamoto, *Confronting the minimal supersymmetric standard model with the study of scalar leptons at future linear* e^+e^- *colliders*, *Phys. Rev.* **D 54** (1996) 6756 [hep-ph/9606370];
M.N. Danielson et al., *Supersymmetry at the NLC* prepared for *1996 DPF/DPB summer study on new directions for high-energy physics (Snowmass 96)*, Snowmass, Colorado, 25 Jun – 12 Jul 1996 SLAC-REPRINT-1996-010
; See also J.L. Feng and M.M. Nojiri, *Supersymmetry and the linear collider*, hep-ph/0210390.